

# **EVALUATION OF HOT MIX ASPHALT MOISTURE SENSITIVITY USING THE NOTTINGHAM ASPHALT TEST EQUIPMENT**

Sponsored by  
the Iowa Highway Research Board  
(IHRB Project TR-483)  
and  
the Iowa Department of Transportation  
(CTRE Project 02-117)



*Center for Transportation  
Research and Education*

Department of Civil, Construction, and Environmental Engineering

IOWA STATE UNIVERSITY

---

---

---

Final Report • July 2005

### **Disclaimer Notice**

The opinions, findings, and conclusions expressed in this publication are those of the authors and not necessarily those of the Iowa Department of Transportation or the Iowa Highway Research Board. The sponsors assume no liability for the contents or use of the information contained in this document. This report does not constitute a standard, specification, or regulation. The sponsors do not endorse products or manufacturers.

### **About CTRE/ISU**

The mission of the Center for Transportation Research and Education (CTRE) at Iowa State University is to develop and implement innovative methods, materials, and technologies for improving transportation efficiency, safety, and reliability while improving the learning environment of students, faculty, and staff in transportation-related fields.

### Technical Report Documentation Page

|   |  |   |                        |
|---|--|---|------------------------|
| <b>1. Report No.</b><br>IHRB Project TR-483   | <b>2. Government Accession No.</b>                                 | <b>3. Recipient's Catalog No.</b>                                   |                        |
| <b>4. Title and Subtitle</b><br>Evaluation of Hot Mix Asphalt Moisture Sensitivity Using the Nottingham Asphalt Test Equipment  |  | <b>5. Report Date</b><br>July 2005                                  |                        |
|   |  | <b>6. Performing Organization Code</b>                              |                        |
| <b>7. Author(s)</b><br>Sunghwan Kim, Brian J. Coree   |  | <b>8. Performing Organization Report No.</b><br>CTRE Project 02-117 |                        |
| <b>9. Performing Organization Name and Address</b><br>Center for Transportation Research and Education<br>Iowa State University<br>2901 South Loop Drive, Suite 3100<br>Ames, IA 50010-8634   |  | <b>10. Work Unit No. (TRAIS)</b>                                    |                        |
|   |  | <b>11. Contract or Grant No.</b>                                    |                        |
| <b>12. Sponsoring Organization Name and Address</b><br>Iowa Highway Research Board<br>Iowa Department of Transportation<br>800 Lincoln Way<br>Ames, IA 50010  |  | <b>13. Type of Report and Period Covered</b><br>Final Report        |                        |
|   |  | <b>14. Sponsoring Agency Code</b>                                   |                        |
| <b>15. Supplementary Notes</b><br>Visit <a href="http://www.ctre.iastate.edu">www.ctre.iastate.edu</a> for color PDF file of this and other research reports  |  |   |                        |
| <b>16. Abstract</b><br><p>Moisture sensitivity of Hot Mix Asphalt (HMA) mixtures, generally called stripping, is a major form of distress in asphalt concrete pavement. It is characterized by the loss of adhesive bond between the asphalt binder and the aggregate (a failure of the bonding of the binder to the aggregate) or by a softening of the cohesive bonds within the asphalt binder (a failure within the binder itself), both of which are due to the action of loading under traffic in the presence of moisture.</p> <p>The evaluation of HMA moisture sensitivity has been divided into two categories: visual inspection test and mechanical test. However, most of them have been developed in pre-Superpave mix design. This research was undertaken to develop a protocol for evaluating the moisture sensitivity potential of HMA mixtures using the Nottingham Asphalt Tester (NAT).</p> <p>The mechanisms of HMA moisture sensitivity were reviewed and the test protocols using the NAT were developed. Different types of blends as moisture-sensitive groups and non-moisture-sensitive groups were used to evaluate the potential of the proposed test. The test results were analyzed with three parameters based on performance character: the retained flow number depending on critical permanent deformation failure (<math>RFN_p</math>), the retained flow number depending on cohesion failure (<math>RFN_c</math>), and energy ratio (ER).</p> <p>Analysis based on energy ratio of elastic strain (<math>ER_{EE}</math>) at flow number of cohesion failure (<math>FN_c</math>) has higher potential to evaluate the HMA moisture sensitivity than other parameters. If the measurement error in data-acquisition process is removed, analyses based on <math>RFN_p</math> and <math>RFN_c</math> would also have high potential to evaluate the HMA moisture sensitivity. The vacuum pressure saturation used in AASHTO T 283 and proposed test has a risk to damage specimen before the load applying.</p> |  |   |                        |
| <b>17. Key Words</b><br>hot mix asphalt—moisture sensitivity—Nottingham Asphalt Tester—stripping  |  | <b>18. Distribution Statement</b><br>No restrictions.               |                        |
| <b>19. Security Classification (of this report)</b><br>Unclassified.  | <b>20. Security Classification (of this page)</b><br>Unclassified. | <b>21. No. of Pages</b><br>65                                       | <b>22. Price</b><br>NA |

# **EVALUATION OF HOT MIX ASPHALT MOISTURE SENSITIVITY USING THE NOTTINGHAM ASPHALT TEST EQUIPMENT**

**Final Report  
July 2005**

**Principal Investigator**

Brian J. Coree

Assistant Professor

Department of Civil, Construction, and Environmental Engineering, Iowa State University

**Research Assistant**

Sunghwan Kim

**Authors**

Sunghwan Kim, Brian J. Coree

Sponsored by  
the Iowa Highway Research Board  
(IHRB Project TR-483)

Preparation of this report was financed in part  
through funds provided by the Iowa Department of Transportation  
through its research management agreement with the  
Center for Transportation Research and Education,  
CTRE Project 02-117.

A report from  
**Center for Transportation Research and Education**

**Iowa State University**

2901 South Loop Drive, Suite 3100

Ames, IA 50010-8634

Phone: 515-294-8103

Fax: 515-294-0467

[www.ctre.iastate.edu](http://www.ctre.iastate.edu)

## TABLE OF CONTENTS

|  |     |
|--|-----|
| ACKNOWLEDGMENTS .....  | VII |
| EXECUTIVE SUMMARY .....  | IX  |
| INTRODUCTION .....   | 1   |
| LITERATURE REVIEW .....  | 3   |
| The Definitions and the Cause of the Moisture Damage of HMA .....                    | 3   |
| The Mechanisms of Moisture Damage in HMA.....  | 6   |
| Reviewing Current Test Methods Used to Predict the Moisture Sensitivity of HMA ..... | 8   |
| Summary and Current Problem State .....  | 11  |
| MATERIALS.....   | 12  |
| Asphalt Binder .....   | 12  |
| Aggregates .....   | 12  |
| Summary .....  | 15  |
| METHODOLOGY .....  | 16  |
| Preliminary Issues .....   | 16  |
| Pilot Study.....   | 20  |
| Final Laboratory Testing Protocol.....   | 21  |
| Summary .....  | 24  |
| ANALYSIS OF TEST RESULTS AND DISCUSSION.....   | 25  |
| Laboratory Test Results .....  | 25  |
| Analysis of NAT Data .....   | 28  |
| Summary .....  | 40  |
| General Discussion on the Air Void Distribution in HMA .....                         | 41  |
| CONCLUSIONS AND RECOMMENDATIONS .....  | 44  |
| Conclusions.....   | 44  |
| Summary .....  | 46  |
| Recommendations.....   | 46  |
| REFERENCES .....   | 47  |
| APPENDIX A: THE TERMINOLOGY OF SUPERPAVE VOLUMETRIC MIX DESIGN .....                 | 51  |
| APPENDIX B: MOISTURE PRE-CONDITIONING SYSTEM RESULTS.....                            | 53  |

## LIST OF FIGURES

|  |    |
|--|----|
| Figure 1. 12.5mm nominal maximum size gradation used .....   | 14 |
| Figure 2. Summary of percentage of accumulated permanent axial strain in repeated load test with NAT ..... | 26 |
| Figure 3. Percentage of accumulated permanent axial strain for each mixture .....                          | 27 |
| Figure 4. Slope of the permanent axial strain in repeated load axial test with NAT .....                   | 29 |
| Figure 5. Slope of the permanent axial strain for each mixture .....                                       | 30 |
| Figure 6. $RFN_p$ for unconditioned and moisture conditioned mixtures .....                                | 31 |
| Figure 7. Resilient modulus in repeated load test for CGS with NAT .....                                   | 34 |
| Figure 8. $RFN_C$ for unconditioned and moisture conditioned mixture .....                                 | 35 |
| Figure 9. ER at $FN_p$ for unconditioned and moisture conditioned mixtures .....                           | 37 |
| Figure 10. ER at $FN_C$ for unconditioned and moisture conditioned mixtures .....                          | 38 |
| Figure 11. Air void distribution in HMA .....  | 42 |

## LIST OF TABLES

|   |    |
|---|----|
| Table 1. Summary of factors influencing moisture damage .....                                       | 6  |
| Table 2. The fine aggregate angularity .....  | 13 |
| Table 3. Specific gravity for each aggregate blend .....  | 13 |
| Table 4. Aggregate gradation .....  | 14 |
| Table 5. Aggregate blends .....   | 15 |
| Table 6. Factors considered in each phase .....   | 16 |
| Table 7. The sequences of changes in asphalt mixture specimen with water and vacuum condition ..... | 18 |
| Table 8. Test conditions in the proposed moisture pre-conditioning system .....                     | 19 |
| Table 9. The result of Superpave mix design for each aggregate blend .....                          | 22 |
| Table 10. The number of gyration for different blended aggregates .....                             | 23 |
| Table 11. NAT test condition used .....   | 24 |
| Table 12. Summary of statistical analysis for suggested parameters .....                            | 40 |
| Table 13. $V_{NP}$ of coarse and dense-graded mixture .....   | 42 |
| Table B.1. Moisture pre-conditioning results for set 1 specimens .....                              | 54 |
| Table B.2. Moisture pre-conditioning results for set 2 specimens .....                              | 55 |

## **ACKNOWLEDGMENTS**

The research was sponsored by the Iowa Highway Research Board (Project TR-483). The support of this board is acknowledged and greatly appreciated.

## EXECUTIVE SUMMARY

Even though moisture sensitivity of Hot Mix Asphalt (HMA) mixtures has been recognized as a major form of distress in asphalt concrete pavements since the advent of asphalt paving technology, the mechanism of this problem has not been clearly identified until now. However, it has been agreed that it can be characterized by the loss of adhesive bond between the asphalt binder and the aggregate or by a softening of the cohesive bonds within the asphalt binder, both of which are due to the action of loading under traffic in the presence of moisture. The evaluation of Hot Mix Asphalt moisture sensitivity has been divided into two categories: visual inspection test and mechanical test. However, most of them have been developed in pre-Superpave mix design. This research was conducted to develop a new test protocol which can overcome the problems of the current procedures and to evaluate the possibility of using the Nottingham Asphalt Tester (NAT) in the resulting procedure.

To achieve these objects, a new test protocol was proposed through a comprehensive literature review. The proposed test protocol was to correspond with Superpave mix design system for sample preparation and to perform the mechanical tests in a manner representing the effect of repeated traffic loading on a pavement on samples in a state (degree of saturation) typical of in situ conditions. In this manner, it was consequently decided that, having induced the appropriate degree of saturation in the sample, it should remain immersed in water throughout ensuing testing (repeated loading test with NAT).

An unmodified PG 58-28 asphalt binder and three types of aggregate (crushed gravel, gravel sand, and fine and coarse crushed limestone) were selected to verify the proposed test. Crushed gravel was used as the coarse “stripping” aggregate and gravel sand was used as the fine “stripping” aggregate. A fine and coarse limestone was considered to be a “non-stripping” aggregate and used as a control. The aggregate blends were selected based on their expected sensitivity to stripping: (1) crushed gravel, (2) 50/50 blend of crushed gravel and crushed limestone, and (3) crushed limestone (in the order of expected moisture sensitivity). In combination with the two gradations (dense and coarse), a total of six blends were used to fabricate sample.

Samples were fabricated at  $7\% \pm 1\%$  air void content by following Superpave volumetric mix procedures. These samples were randomly selected and divided into a dry conditioning group and a moisture conditioning group. The dry conditioning group was directly tested using the repeated load test in the NAT. These samples were tested in water, but sealed from the water by a membrane. The moisture conditioning group was pre-saturated at three different levels of saturation by vacuum conditioning and then tested in the NAT.

Three analytical approaches—flow number, cohesion-friction failure, and fracture energy—were applied to test data to determine the critical transition from sound to unsound for each tested mixture. Three different parameters—the retained flow number depending on critical permanent deformation failure ( $RFN_P$ ), the retained flow number depending on cohesion failure ( $RFN_C$ ), and energy ratio (ER)—were suggested to evaluate the relative sensitivity for different types of blends with different treatments. Visual observation of the exposed fractured faces of tested



specimens and statistical analysis were conducted in order to identify that these observations indeed reflected HMA moisture sensitivity.

Analysis based on energy ratio of elastic strain ( $ER_{EE}$ ) at flow number of cohesion failure ( $FN_C$ ) has a higher potential to evaluate the HMA moisture sensitivity than other parameters. When removing the measurement error in data-acquisition process, analyses based on  $RFN_P$  and  $RFN_C$  would also have high potential to evaluate the HMA moisture sensitivity. The stripping of aggregate was not clearly evident by visual inspection. It appears that the failure of a specimen therefore derives from a cohesive failure in binder, not binder stripping failure from aggregate. Even though there was statistical difference between the dry and the different saturation level mixtures, there was no statistical difference within different saturation level mixtures due to sample damaged through the vacuum pressure saturation before loading tests.

## INTRODUCTION

Moisture sensitivity of Hot Mix Asphalt (HMA) mixtures, generally called stripping, is a major form of distress in asphalt concrete pavement. This problem has been recognized since the advent of asphalt paving technology (1). It is characterized by the loss of adhesive bond between the asphalt binder and the aggregate (a failure of the bonding of the binder to the aggregate) or by a softening of the cohesive bonds within the asphalt binder (a failure within the binder itself), both of which are due to the action of loading under traffic in the presence of moisture. This distress generally begins at the bottom of a sealed HMA layer and progresses upward. Without opening up the pavement and observing the material removed, stripping is usually difficult to identify from surface examination alone. Therefore, the potential for moisture sensitivity in HMA has traditionally been evaluated through laboratory testing.

Factors affecting moisture sensitivity of HMA have been identified as the type and use of the mix, the characteristics of the asphalt binder and the aggregate and environmental effects during and after construction, and the use of anti-stripping additives (2, 4, and 5). Many factors are involved in moisture sensitivity of HMA, so the test method should closely simulate the real field condition to reflect these variables.

Methods in current use have been developed in the pre-Superpave era (i.e., before 1993). Typically, 4 in. diameter by 2.5 in. high impact compacted samples are used. In spite of significant changes in the mix design process, there has been little effort to verify whether the use of 150 mm diameter by 115 mm high Superpave gyratory compacted samples provides the same results and conclusions. A further major problem in all current laboratory methods is the inability of representing real pavement conditions under which stripping occurs. Under real traffic conditions, water damage in asphalt pavement occurs when repeated traffic loading is applied to a saturated pavement, inducing water movement or pressure transients in the void structure of HMA. However, some traditional tests (e.g., ASTM D3625) do not address sample traffic loading or apply a quasi-static loading.

The Nottingham Asphalt Tester (NAT) is widely used in Europe for testing asphalt mixtures. This equipment is specially designed to perform a variety of tests on asphalt mixtures and can apply static and dynamic, confined and unconfined loading to samples under strict temperature control. In addition, this equipment can be readily adapted to test water-saturated or submerged samples. The Iowa DOT has requested that the NAT be used in this project. The Iowa Department of Transportation (Iowa DOT) obtained the NAT, so that any test methods developed at ISU may be readily and directly implemented at the Iowa DOT Office of Materials testing laboratory.

The goal of this research is to develop a protocol for evaluating the moisture sensitivity potential of HMA mixtures using the Nottingham Asphalt Tester. This research seeks to fulfill two specific objectives: (1) to develop a new test protocol which can overcome the problems of the current procedures and (2) to evaluate the possibility of using the Nottingham Asphalt Tester.

To accomplish these goals and objectives, the project was broken into six tasks: (1) conduct a comprehensive literature review, (2) collect and characterize the materials to be used, (3) undertake a pilot study, (4) perform laboratory tests on laboratory prepared samples, (5) analyze the results of using existing theories on moisture damage in HMA mixtures, and (6) make recommendations.

## **LITERATURE REVIEW**

Even though moisture sensitivity of HMA mixtures has been researched for decades, it has proven to be very difficult to confidently predict this type of distress in the laboratory because of factors involved. In this chapter, a comprehensive survey of the literature about stripping in HMA is presented. There are three distinct parts to this search:

1. Examining the history and the causes of moisture damage in HMA
2. Identifying the suggested mechanisms of moisture damage in HMA
3. Reviewing current test methods used to predict moisture sensitivity in HMA

A comprehensive literature search was conducted by using the Transportation Research Information Service (TRIS) database. The leading asphalt journals (e.g., those of the Association of Asphalt Paving Technologists [AAPT], the American Society for Testing and Materials [ASTM], the Highway Research Board [HRB], and the Transportation Research Board [TRB]) were also searched.

The information obtained from the literature review for each of the three topics is discussed at length below.

### **The Definitions and the Cause of the Moisture Damage of HMA**

Since moisture damage in HMA mixtures was first identified as a distress type, a significant amount of effort has been applied to defining the underlying mechanisms and to developing tests to predict its occurrence. Moisture damage in HMA may be generically defined as the separation of the asphalt coating from the aggregate in a compacted HMA mixture in the presence of water under the action of repeated traffic loading.

Overall, two areas of focus have been identified: a failure of bonding of the binder to the aggregate (i.e., a failure of adhesion) and a failure within the binder itself (i.e., a failure of cohesion). These two areas have, over the years, generated a significant body of research leading to a number of disparate conclusions.

#### *Adhesive Failure*

Most researchers, however, consider that moisture damage in HMA is due more to the adhesive mode of failure than to the cohesive mode. For example, as Majidzadeh (6) stated, "...stripping of the binder from aggregate in presence of water (i.e., moisture damage) results in adhesive failure which is considered as an economic loss and an engineering failure in the design of a proper mixture." Kennedy (7) explained that stripping was the loss of adhesion between the asphalt binder and the aggregate due to the action of water, and Tunicliff (8) suggested that stripping was the displacement of the asphalt binder film from the aggregate surface, which he explained using the chemical reaction theory of adhesion. Thus, a number of hypotheses relative to the adhesive bond between asphalt and aggregate have been developed in order to better understand the phenomenon of stripping under this definition.

Hicks (5) provided an overview of previous research on adhesion. He identified four broad theories that have been developed to explain the adhesion of asphalt binder to aggregate.

**Mechanical adhesion** theory (9, 10) suggests that the adhesion of asphalt binder to the aggregate is affected by several aggregate physical properties, including surface texture, porosity or absorption, surface coatings, surface area, and particle size. In general, a rough, porous surface had a tendency to provide the strongest interlock between aggregate and asphalt. However, as Hicks (5) stated, "...the greater the surface area of the aggregate, the greater the amount of asphalt cement required for stability. ....Consequently, a mixture with substantial fines tends to strip more readily because complete particle coating requires more asphalt cement which is more difficult to achieve without creating a stability problem."

**Chemical reaction** between the asphalt binder and the aggregate has been generally accepted to explain why different types of aggregate demonstrate different degrees of adhesion between the binder and the aggregate in the presence of water. In other words, the surface pH values of the aggregate and of the binder affect the quality of the surface adhesion (11). The reason for this has been attributed to the different polarities of the surface minerals in the aggregate and the asphalt binder. In the interior of a crystal, forces are in equilibrium. On the surface of a crystal, the bonding forces of the atoms or molecules may be partially unsatisfied, with excess or "free" charges, so that the surface may exhibit polarity (10). A quartz ( $\text{SiO}_2$ ), which is a primary mineral component of quartzite and other silicious minerals, comprises the silicon dioxide tetrahedron ( $\text{SiO}_4^{4-}$ ) as a unit crystal structure. The silicon atom has a positive valence of 4 and each oxygen atom has a negative valence of 2. The positive valence of the silicon atom is satisfied by sharing its electron with the electron of each oxygen atom. However, one unsatisfied negative valence of each oxygen atom results in a net negative polarity of the quartz crystal structure (10). The surface of calcite ( $\text{CaCO}_3$ ), which is a primary mineral component of limestone, has a non-polar property. This is also related to the crystal structure of calcite. In this structure, the positive valences of the carbon and the calcium atoms are satisfied by the covalent bond with two oxygen atoms and one oxygen atom (e.g.,  $\text{CaCO}_3 \rightarrow \text{CaO} + \text{CO}_2$ ). The satisfied valence of each atom makes the surface of a calcite polyhedron non-polar (12).

**The differential degree of wetting of the aggregate** by asphalt and water has been explained using surface energy theory. Rice (10) suggested that when asphalt and aggregate were brought together, adhesion tension is established between two phases. He also reported data which indicated that the adhesion tension for water-to-aggregate is higher than that for asphalt-to-aggregate. Hicks stated, "... water will tend to displace asphalt cement at an aggregate-asphalt cement interface where there is contact between the water, asphalt, and aggregate." Mark (14) indicates that interfacial tension between the asphalt and aggregate varies with both the type of aggregate and the type of asphalt cement.

**Molecular orientation** theory affirms that when asphalt binder comes into contact with an aggregate surface, the molecules in the asphalt align themselves on the aggregate surface to satisfy the energy demand of the aggregate (15). It was demonstrated that this alignment of asphalt molecules was affected by the orientation of unsatisfied ions on the surface of aggregate, (14). Hicks stated, "...water molecules are dipolar. Asphalt molecules are generally non-polar,

although they contain some polar components. Consequently, water molecules, being more polar, may more readily satisfy the energy demands of an aggregate surface.”

### *Cohesive Failure*

Even though cohesive failure of asphalt has been regarded as a less important factor in the definition of moisture damage of HMA, Bikerman (16) suggested that the probability of cohesive failure was much greater than of adhesive failure. This was also demonstrated by work of Kanitpong and Bahia (17), which is supported by the observation of failure surfaces in asphalt mixtures obtained from the Tensile Strength Ratio (TSR) test, where the failure was visually observed within the binder coating without evidence of apparent loss of adhesion to the aggregate particles.

This cohesive failure can be partially explained by emulsification of water in the asphalt phase, which is different to conventional emulsified asphalts in which the asphalt is emulsified in a water phase (28). Fromm’s work (28) showed that water could enter into the asphalt film and form a water-in-asphalt emulsion. This emulsification of water in the asphalt film causes asphalt particles to separate from the asphalt film (cohesive failure) and ultimately leads to an adhesive failure at a critical time when this emulsification boundary propagates to the aggregate surface.

However, since the mechanism of cohesive failure leads, ultimately, to an adhesive failure, most instances of cohesive failure may only be inferred rather than observed, and the final mechanism (i.e., adhesive) is reported as the cause (18). Thus, even though the definition of moisture damage in HMA has been regarded as the failure of adhesive and cohesive bonds between the asphalt and the aggregates in the presence of water, it has proven difficult to distinguish between the two modes of failure in predicting failure mode unless the failure surface of HMA is visually inspected a posteriori (18).

### *Factors Influencing Moisture Damage in HMA*

Several surveys (2, 4, and 5) have been undertaken to better understand which factors should be considered in evaluating moisture damage in HMA mixtures. Many variables, including the type and use of the mix, asphalt characteristics, aggregate characteristics, environmental effects during and after construction, and the use of anti-stripping additives (2, 4, and 5), have been identified. Even though most responses in these surveys were as expected, some results were contradictory. For example, gravel is not always associated with stripping. The reason for this was pointed out in the literature: even though the chemistry of the original gravel deposit made it moisture susceptible, compounds that could prevent stripping might be adsorbed into the aggregate surfaces over a period of geologic time so that the same gravel might exhibit good resistance to stripping, unless it was crushed and thereby exposed “fresh” surfaces to the asphalt (8).

Based on work by Hicks (4), Table 1 summarizes the factors influencing moisture damage.

**Table 1. Summary of factors influencing moisture damage**

| <b>Factor</b>                               | <b>Desirable Characteristics</b>               | <b>Supporting Researchers</b>                         |
|---|--|---|
| 1) Aggregate                                |  |   |
| a) Surface Texture                          | Rough  | Hicks (5), Majidzadeh and Brovold(6)                  |
| b) Porosity                                 | Depends on pore size                           | Hicks (5),Thelen (19)                                 |
| c) Mineralogy                               | Basic (PH=7) Aggregate are more resistant      | Rice (10), Majidzadeh and Brovold(6)                  |
| d) Dust Coatings                            | Clean  | Majidzadeh and Brovold (6),<br>Tunncliff and Root (8) |
| e) Surface Moisture                         | Dry  | Majidzadeh and Brovold (6), Kim, Bell and Hicks (20)  |
| f) Surface Chemical Composition             | Able to share electrons or form hydrogen bonds | Hicks (5)   |
| g) Mineral Filler                           | Increase viscosity of Asphalt                  | Hicks (5)   |
| 2) Asphalt Cement                           |  |   |
| a) Viscosity                                | High   | Thelen (19),Schmit and Graf (20)                      |
| b) Chemistry                                | Nitrogen and Phenols                           | Curtis et al. (22)                                    |
| C) Film Thickness                           | Thick  | Hicks (5)   |
| 3) Type of Mixture                          |  |   |
| a) Voids                                    | Very low or Very high                          | Terrel and Shute (23)                                 |
| b) Gradation                                | Very dense or Very open                        | Brown et al. (24), Takallou et al. (25)               |
| c) Asphalt Content                          | High   | Hicks(5)  |
| 4) Environmental Effect During Construction |  |   |
| a) Temperature                              | Warm   | Hicks (5), Majidzadeh and Brovold (6)                 |
| b) Rainfall                                 | None   | Hicks (5)   |
| c) Compaction                               | Sufficient                                     | Hicks (5), Tunncliff and Root (8)                     |
| 5) Environmental Effect after Construction  |  |   |
| a) Rainfall                                 | None   | Hicks (5)   |
| b) Freeze–Thaw                              | None   | Lottman (26), Taylor and Khosla (27)                  |
| c) Traffic Loading                          | Low Traffic                                    | Fromm (28), Gzowski et al. (29)                       |
| 6) Modifiers or Additives                   | Use  | Tunncliff and Root (8)                                |

### **The Mechanisms of Moisture Damage in HMA**

Even though many factors have been suggested to influence moisture damage in HMA mixtures, the essential problem was how water penetrated the asphalt film and/or interfaces between asphalt and aggregate. Several different mechanisms have been identified in the literature.

Rice (10) and Thelen (19) approached this problem by using a proposed adhesion mechanism such as surface energy theory and chemical reaction between asphalt binder and aggregate. Surface energy theory suggested that the differential amount of interfacial tension and work of

separation between pure asphalt, water, and aggregate resulted in an adhesion failure between the asphalt and aggregate (10, 19). Why stripping was observed more in quartz than limestone is answered by the differential chemical reactivities between the asphalt and aggregate. Water is a polar molecule and asphalt is either non-polar or weakly polar. In addition, molecules of silica and silicates have high dipole moments (higher than that of water), and carbonate rocks are also polar to limited degree. Thus, siliceous aggregates such as quartz can adsorb more water than asphalt because of the attraction between the polar mineral molecules and the polar water molecules. Furthermore, on a relatively non-polar surface, such as limestone, the cohesive forces in the water are greater than the adhesive forces between water and limestone. Therefore, a weakly polar substance such as asphalt does not preferentially strip from limestone and is held to the surface primarily by van der Waal's forces (10).

Fromm (28) pointed out, "... Thelen did not explain where or how all of the values used for the various interfacial tensions in surface energy theory were obtained." He focused on how and where water penetrated the asphalt film and diffused into the remaining asphalt and onto the aggregate surface. He suggested and demonstrated the emulsification of water in asphalt and the rupture (degradation) of the coating film (28). Fromm explained that the asphalt film can be ruptured (degraded) due to the different amount of interfacial tension in many air-water-asphalt junctures which are formed when water enters the HMA mixture. The rupture of the asphalt film reduces the effective film thickness of the asphalt so that the emulsified water can move relatively rapidly to the aggregate surface (28).

Lottman tried more closely to replicate field-related conditions in the laboratory. To carry out this project (30, 31), he took notice of the behavior of water in the pore structure of an HMA mixture loaded by heavy traffic. He suggested some of the major moisture-damage mechanisms (26):

1. The development of pore water pressure in the mixture voids due to the repetition of wheel-loads; thermal expansion and contraction produced by ice formation, temperature cycling above freezing, freeze-thaw, and thermal shock; or a combination of these factors (mechanical disruption)
2. Asphalt removal by water in the mixture at moderate to high temperatures (emulsification)
3. Water-vapor interaction with the asphalt filler mastic and larger aggregate interfaces (adhesion failure based on surface energy theory)
4. Water interaction with clay minerals in the aggregate fines (adhesion failure based on chemical reaction)

Based on these hypotheses, he developed a mechanical laboratory test protocol generally referred to as the Lottman test. The exposed interiors of laboratory tested specimens were compared to those of field damaged specimens and this was used to confirm the Lottman test protocol and hypothesis (30).

Hydraulic scouring has been suggested to explain moisture damage due to the movement of surface traffic loads on saturated HMA pavement. When a heavy traffic wheel moves over a saturated pavement surface, water is pressurized within the pavement void structure in front of



the moving load and immediately relieved behind the load. Thus, sealed surface layers, where the traffic-imposed loads are highest, were stripped by rapidly reversing high water velocities and pressures within the saturated pore structure (27). However, it has been generally observed by inspection of field specimens of stripped pavements that most stripping begins at the bottom of an HMA layer and progresses upwards (3). Taylor and Khosla (27) suggested that the reason for this behavior was that the asphalt at the bottom of a pavement layer is usually in tension under the application of surface applied loads and is often influenced by prolonged exposure to moisture from water trapped within a granular base course above the subgrade.

Kandhal (3) also recognized inadequately drained granular base as supply of water to saturated HMA pavement layers. Water in inadequately drained granular bases is transferred into the HMA pavement layer in the form of water or water vapor during the heat of the day. This water vapor condenses at night so that the HMA pavement layers become saturated.

### **Reviewing Current Test Methods Used to Predict the Moisture Sensitivity of HMA**

The development of tests to predict the potential of moisture sensitivity of HMA began in the 1930s (23). Since that time, numerous tests have been developed to identify moisture sensitivity of HMA mixtures. Hicks (5) stated that failure due to the moisture damage to HMA occurs in two stages. The first stage is the failure of the adhesion and cohesion bonds and the second stage is the mechanical failure of the pavement under traffic action, as a logical continuation of the first stage. Thus, tests were separated into three categories depending which stage is deemed more critical in moisture damaged HMA pavement.

- Visual inspection testing focuses on the first stage failure. The loose mixture is immersed in water at room temperature or boiling water for a specific duration. The criteria of failure are decided by visual identification of stripped (uncoated) aggregate.
- Mechanical laboratory testing considers the second stage failure as more detrimental in HMA pavements. The compacted mixture is conditioned in a manner that is intended to simulate the real situation. A comparison of the physical conditions such as strength or resilient modulus of the conditioned and unconditioned samples is used to evaluate the moisture sensitivity potential in HMA pavement.
- Loaded wheel testing simulates in the laboratory the pavement under traffic. This testing was originally developed to evaluate rutting in asphalt mixtures. However, it has been recognized that when these tests are performed on saturated mixtures, there is a possibility to more accurately evaluate moisture sensitivity in HMA.

Even though numerous test have been proposed, only the following tests have become national standards and are in common use by public agencies (32, 33).

#### ***Boiling Water Test—ASTM D 3625***

Loose HMA is added to boiling water for 10 minutes and the percentage of the total visible surface area of aggregate that retains its original coating after boiling is estimated. If this value is below 95%, it is considered that this HMA has the potential to fail by stripping. This test has

been modified by considering various methods of stirring the mixture, various sample sizes, and various procedures for adding water (4).

*Static Immersion Test—ASTM D 1664, AASHTO T182*

A specimen of HMA mix is immersed in distilled water at 77°F for 16 to 18 hours and is observed under water to visually estimate the total surface area of the aggregate on which asphalt coating remains.

*Indirect Tensile Test and/or Modulus Test—ASTM D 4867, AASHTO T 283*

Lottman (30, 31) developed an indirect tensile test to predict the moisture sensitivity of HMA under “real traffic service” conditions. One-third of the prepared sample is kept in the dry condition. After exposing the remaining two-thirds of the samples to vacuum saturation, one half of the vacuum saturated samples are exposed to secondary conditioning consisting of a single freeze–thaw cycle (0°F–140°F) or repeated freeze–thaw cycles (18 cycles of 0°F–120°F–0°F). After the two sample groups—dry conditioned and moisture conditioned—are tested for indirect tensile strength and instantaneous E-modulus at 55°F and 73°F, the data are normalized by expressing them in the form of a tensile strength ratio (TSR) and an E-modulus ratio (E-MODR), where the tensile strength and E-modulus of the conditioned specimens are expressed as percentages of the dry (unconditioned) results (30). Field evaluation (31), involving 17 in-service pavements in 14 states, indicated that a minimum tensile strength ratio of 0.7 provided good reliability in identifying good stripping resistance.

Schmidt and Graf (35) evaluated moisture susceptibility by applying various moisture conditioning schemes and using resilient modulus. The value of the resilient modulus was calculated from the loading and deformation values, the sample thickness, and an assumed value of Poisson’s ratio by applying a 0.1 sec duration indirect pulse load. The resilient modulus is used as a design parameter in flexible pavement design and provides a great potential for correlating moisture damage observed in the laboratory with field performance (27).

Tunnicliff and Root (8) criticized Lottman’s method by pointing out that the induced damage could be attributed to the conditions of the test rather than to the moisture susceptibility of the mixtures tested. Thus, conditioning after vacuum saturation was modified to simulate more accurate locally prevalent climatic conditions.

AASHTO T283 (33), which is generally referred to as the “modified Lottman” test, was developed by Kandhal and adopted by AASHTO in 1985 (3). It is a combination of the Lottman and the Root-Tunnicliff tests. Work by Kiggunndu and Roberts indicate this test is the most accurate test method currently available for predicting moisture damage in HMA mixtures (2).

*Immersion and Compression Test—AASHTO T 165, ASTM D1075*

Even though this method is a mechanical test similar to the indirect tensile test and/or modulus test, the main differences relate to the manner of sample compaction (double plunger vs.

Marshall impact) and a mechanical test used (indirect compression vs. indirect tension or resilient modulus). In this approach, the ratio of retained indirect compressive strengths between the conditioned and unconditioned samples is used as the acceptance criterion.

#### *Net Adsorption Test (NAT) and Environmental Conditioning System (ECS)*

Studies on the moisture susceptibility in HMA have been further developed by two Strategic Highway Research Program (SHRP) projects—SHRP A-003A “Performance Related Testing and Measuring of Asphalt–Aggregate Interactions and Mixtures” and SHRP A-003B “Fundamental Properties of Asphalt–Aggregate Interactions Including Adhesion and Adsorption.” The products of these studies are the Environmental Conditioning System (ECS) and the Net Adsorption Test (NAT—not to be confused with the Nottingham Asphalt Tester [NAT]).

The ECS (18), a product of SHRP project A-003A which developed a moisture susceptibility test having a wide capability to simulate field condition, consisted of three subsystems, such as fluid conditioning, an environmental conditioning cabinet, and a loading system. In these subsystems, an HMA sample experienced various conditioning cycles that were intended to simulate real field conditions. After conditioning, the modular ratio, water permeability, and percent stripping based on visual inspection are used to evaluate the moisture susceptibility of HMA.

The Net Adsorption Test (37) was developed through the SHRP project A-003B that focused on the fundamental aspects of the bond between aggregates and asphalt binders. A solution of asphalt in toluene is added to an aggregate sample and subsequently removed after specific times with or without the introduction of further water. The differential amount of absorption of asphalt into the aggregate from asphalt/toluene solution between the “with water” and “without water” cases can be measured using the difference in the amount of asphalt binder concentration from the supernatant solution. This test determines aggregate potential for moisture sensitivity.

#### *Traffic Simulation Testing*

The loaded condition on pavement derives from the passage of traffic wheel loads passing over the pavement surface. Even though most performance tests have been developed to simulate this condition through many hypotheses, only several tests closely simulate this condition. The common element of these tests is the application of a wheel loading over the surface of the sample. Some of these include the Asphalt Pavement Analyzer (APA), the Georgia Loaded Wheel Tester (GLWT), and the Hamburg Wheel Tracking Device (HWTd).

Among these, the HWTd has been used to evaluate rutting and stripping in Germany (46). In the evaluation of stripping using the HWTd, a rectangular slab specimen (10.2 x 12.6 x 1.6 in) is compacted to  $7\% \pm 1\%$  air voids using a laboratory rolling compactor and tested with a 47 mm wide steel wheel under a load of 705N. The wheel is moved back and forth over the specimen while submerged under water. The results are plotted on a graph of the permanent deformation (rut depth) versus the number of wheel passes. As the number of wheel passes increases, the permanent deformation increases slowly until at some point a rapid increase in the rate of

deformation is observed. A bi-linear plot is observed, and it has been hypothesized that the point at which the slopes change (referred to as the stripping inflection point) indicates the initiation of stripping within the mixture. The number of loaded wheel passes needed to achieve the stripping inflection point is used as a relative measure of susceptibility to stripping. Unfortunately, the various equipment used (i.e., Asphalt Pavement Analyzer, Hamburg Wheel Tracking Device, and Georgia Loaded Wheel Tester) rank mixtures differently with respect to moisture susceptibility.

## **Summary and Current Problem State**

The objective of this literature review was (1) to examine how the moisture damage of HMA has been defined and the causes of this phenomenon; (2) to identify how water causes damage in HMA; and (3) to review test methods used to evaluate moisture sensitivity in HMA. The result of this review may be summarized as follows:

1. Moisture damage in HMA can be defined as the separation of asphalt and aggregate in the presence of water under traffic loads. Various mechanisms are ascribed to this phenomenon.
2. Competing mechanisms of moisture damage in HMA mixtures have been developed from an examination of the fundamental aspects of the attractive forces between asphalt and aggregate surfaces.
3. Many suggested tests have provided various simulations based on many of the identified mechanisms of moisture damage in HMA mixtures.

Even though various concepts of moisture damage of HMA have been suggested, the conclusion is that individually these concepts cannot explain all occurrences of moisture damage in HMA mixtures. In addition, it is difficult to discriminate between competing mechanisms when evaluating actual failure due to stripping.

It has been hypothesized that a mechanical test is a necessary element in estimating the moisture damage problem. This is supported by other researchers works (5, 6), which evaluated moisture sensitivity various tests. Their work demonstrated that the modified Lottman test (AASHTO T 283) and the Root-Tunnicliff test (ASTM D 4867) were more effective than the Boiling water test (ASTM D 3625) and the Static immersion test (ASTM D 1664). In spite of actual simulation of traffic wheel loading passing on pavement, current developed traffic simulation tests have not clearly identified that the failure of tested specimen comes from the moisture damage or other distress (rutting). In addition, the precision of tests has not yet been developed.

## **MATERIALS**

Material selection is an important component of this study. This work was carried out with the cooperation of Iowa DOT Bituminous Materials Engineer and his staff. The type of asphalt binder was accepted as a fixed variable, while more effort was focused on the selection of the aggregates so that gravel and a coarse gradation were selected as moisture-sensitive factors and limestone and a dense gradation as non-moisture-sensitive factors.

### **Asphalt Binder**

The binder was selected to be a PG 58–28 grade asphalt binder, produced by Jebro Inc. of Sioux City, Iowa. It was selected as it is in common use in the state of Iowa. The binder tests were conducted following American Association of State Highway and Transportation Officials (AASHTO) MP1 specification requirements. The complete discussion of these results is provided by Kim (47).

### **Aggregates**

It was deemed important to consider aggregates that are known to be “strippers” and also to use a “non-stripper” as a control. Three types of aggregates were selected: a crushed gravel, a gravel sand, and a fine and coarse crushed limestone. Hallet Materials Co, Iowa, supplied crushed gravel as the coarse “stripping” aggregate and a gravel sand as the fine “stripping” aggregate. Both the coarse and fine crushed lime stones were obtained from Martin–Marietta Aggregate of Ames, Iowa. However, the gravel fine aggregate was deficient in fines so that some natural gravel from Automated Sand and Gravel of Fort Dodge, Iowa, and some crushed limestone filler was used to supplement this deficiency. However, it was necessary to compare the effects of these substitutions. The repeated loading test in NAT was undertaken for two materials—a lime stone filler and a gravel filler—at the same degree of saturation. From this testing, it was noted that limestone used as a filler ( $P_{200}$ ) is more sensitive to moisture than a gravel filler (47). It is clear that this use of crushed limestone filler was not providing an anti-strip function within the overall mixture.

### *Aggregate Properties*

Two sets of aggregate property requirements—consensus properties and source properties—were provided in Superpave system. The use of Martine–Marietta crushed limestone would normally be permitted in HMA mixtures under Iowa DOT specifications so that they might meet all of source properties and consensus properties. While the use of the Hallett gravel aggregates (rounded alluvial deposits) would not normally be permitted in HMA mixtures under Iowa DOT specifications, it was accepted that while they might meet the source property requirements, they might not meet all of the consensus properties. Thus, it did not feel the conducting all of test required in Superpave system.

Fine aggregate angularity test, which is the one of the aggregate consensus property tests in Superpave system, was undertaken for each blended aggregate. The results of the fine aggregate angularity tests are reported in Table 2.

**Table 2. The fine aggregate angularity**

|                        | <b>Limestone</b> | <b>Gravel</b> | <b>50/50</b> |
|------------------------|------------------|---------------|--------------|
| Dense-graded blending  | 41.1             | 37.1          | 39.4         |
| Coarse-graded blending | 41.1             | 36.1          | 39.1         |

The aggregate specific gravity for each aggregate blend is needed to design Superpave HMA mixtures. The Corelock™ System was used to determine the specific gravity in Table 3.

**Table 3. Specific gravity for each aggregate blend**

|                        | <b>Lime stone</b> | <b>Gravel</b> | <b>50/50</b> |
|------------------------|-------------------|---------------|--------------|
| Dense-graded blending  | 2.652             | 2.621         | 2.632        |
| Coarse-graded blending | 2.656             | 2.623         | 2.638        |

A nominal maximum aggregate size of 12.5 mm (0.5 in) was selected as a typical Iowa mixture. Two dense and one coarse gradations were also selected. These gradations have been used in asphalt pavement construction in Iowa and could be obtained with the help of the Iowa DOT Office of Materials. The difference between the two dense gradations is only in the amount of passing 75 micron ( $P_{200}$ ): 4% and 5%. Even though the gravel sand was used in this study to compare the moisture sensitivity in different types of aggregate, the gravel sand would not normally be permitted in asphalt paving mixtures. When 5%  $P_{200}$  material in the dense gradation was used to decide optimum binder content, the character of asphalt mixes at optimum binder content couldn't satisfy the criteria of Superpave volumetric mix design, so 4% of passing 75 micron ( $P_{200}$ ) was used in the dense gradation of the gravel sand blended aggregates. Even though the amount of passing 75 micron ( $P_{200}$ ) was different, the amount of passing the other size was not significantly changed. Washed aggregate fractions were carefully proportioned in the laboratory to meet the selected target gradations, as shown in Figure 1 and Table 4.

**Table 4. Aggregate gradation**

| Sieve No.(mm) | Percent Passing 12.5 mm NMA |          |           |
|---------------|-----------------------------|----------|-----------|
|               | Coarse                      | Dense 1* | Dense 2** |
| 19            | 100                         | 100      | 100       |
| 12.5          | 92                          | 92       | 92        |
| 9.5           | 82                          | 82       | 82        |
| 4.75          | 51                          | 58       | 57        |
| 2.36          | 32                          | 41       | 41        |
| 1.18          | 24                          | 31       | 31        |
| 0.600         | 17                          | 22       | 21        |
| 0.300         | 10                          | 13       | 12        |
| 0.150         | 7                           | 8        | 7         |
| 0.075         | 5                           | 5        | 4         |

\* The aggregate blend using all of limestone as fine aggregate

\*\* The aggregate blend using all of gravel sand or half of gravel as fine aggregate

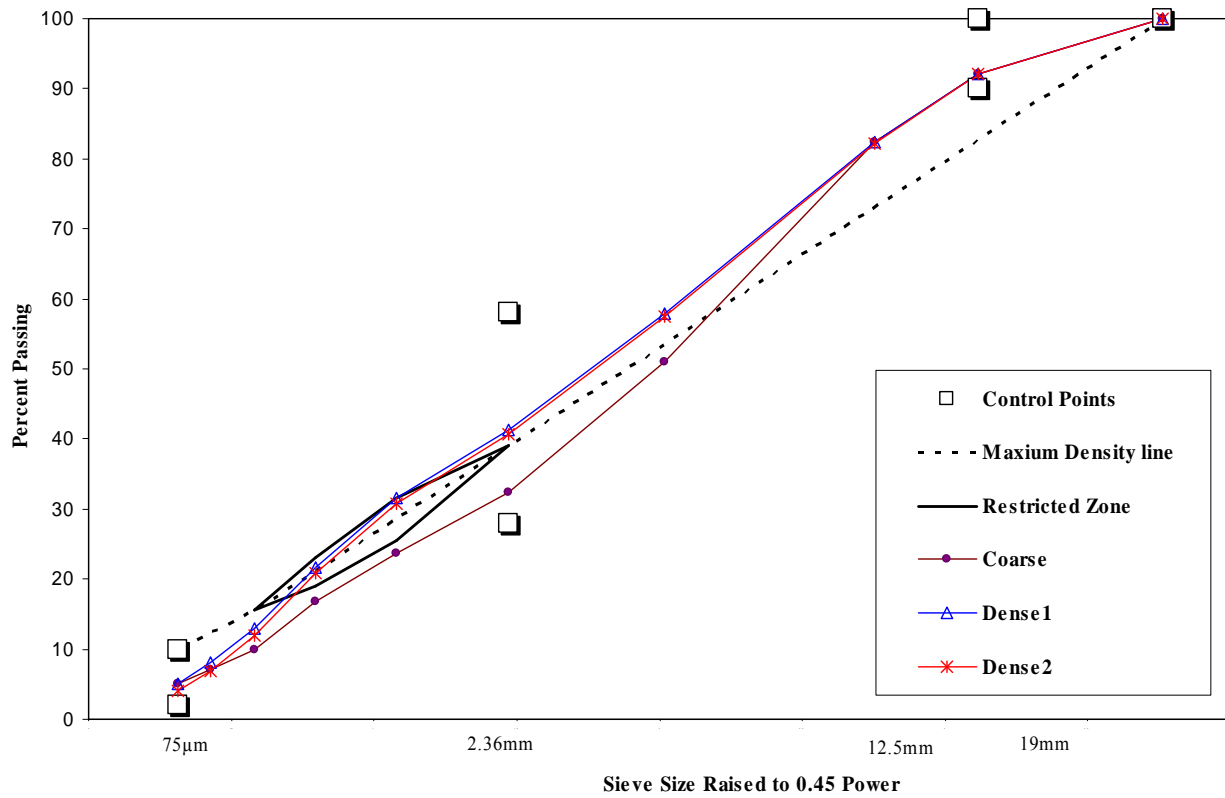


**Figure 1. 12.5mm nominal maximum size gradation used**

### *Aggregate Blends*

The aggregate blends were selected based on their expected sensitivity to stripping—a crushed gravel, a 50/50 blend of crushed gravel and crushed limestone, and a crushed limestone—in the order of expected moisture sensitivity. In combination with the two gradations, a total of six blends were available. However, crushed limestone fines passing 75 micron ( $P_{200}$ ) were used as the fine aggregate passing 75 micron ( $P_{200}$ ) in all blends. The blends selected are listed in Table 5.

**Table 5. Aggregate blends**

| ID    | Gradation | Material                  |                           |                        |
|-------|-----------|---------------------------|---------------------------|------------------------|
|       |           | Coarse Aggregate          | Fine aggregate            | $P_{200}$              |
| CLL   | Coarse    | Crushed limestone         | Crushed limestone         | Crushed limestone (5%) |
| DLL   | Dense 1   | Crushed limestone         | Crushed limestone         | Crushed limestone (5%) |
| C5050 | Coarse    | Half of crushed limestone | Half of crushed limestone | Crushed limestone (5%) |
|       |           | Half of crushed gravel    | Half of gravel sand       |                        |
| D5050 | Dense 2   | Half of crushed limestone | Half of crushed limestone | Crushed limestone (4%) |
|       |           | Half of crushed gravel    | Half of gravel sand       |                        |
| CGS   | Coarse    | Crushed gravel            | Gravel sand               | Crushed limestone (5%) |
| DGS   | Dense 2   | Crushed gravel            | Gravel sand               | Crushed limestone (4%) |

### **Summary**

The first step in this project was to select the aggregates and asphalt binder. The next step was to characterize these materials through specified tests. An unmodified PG 58–28 asphalt binder was selected. Six types of blended aggregate (three materials blends by two gradations) were used.



## METHODOLOGY

Having selected and characterized the materials to be used, the next question to be answered related to what laboratory procedure could be developed to best satisfy the concerns raised from the literature review, i.e., the need to develop a moisture susceptibility test compatible with the Superpave Mix Design system and real traffic and environmental conditions. To address these problems, the laboratory testing effort was divided into three phases: sample preparation (compaction), sample pre-conditioning, and test evaluation. However, an initial, preliminary phase was deemed necessary to define various material and procedural parameters.

### Preliminary Issues

In setting out to develop a new test protocol, it is necessary to pre-define various parameters and to test these out in a pilot test prior to implementing a more complete study. In this way, practical problems that might subsequently arise during the main experiment would, hopefully, be avoided. Factors considered in this preliminary stage are summarized in Table 6.

**Table 6. Factors considered in each phase**

| <b>Phase</b>             | <b>Factors</b>   |
|--------------------------|--|
| 1. Sample preparation    | Type of Asphalt<br>Type of Aggregate<br>Gradation<br>Air void<br>Specimen size |
| 2. Moisture conditioning | Vacuum Saturation  |
| 3. Evaluation testing    | Type of test in NAT<br>Test condition  |

#### *Sample Preparation (compaction)*

Because it was considered necessary to develop a laboratory testing procedure that will be compatible with the Superpave mix design system, the general approach to sample preparation was to follow Superpave mix design procedures (41) as closely as possible. Material-related factors have been discussed in the previous chapter. Sample compaction was to be undertaken using the Superpave Gyratory Compactor (SGC). The target mixture air void content is an important factor in Superpave mixture evaluation, as well as in any test for moisture susceptibility. Terrel and Shute (18) suggested that any value between the two extremes of total impermeability and free-draining would be detrimental in HMA because moisture could be entrapped in the HMA. Although HMA mixtures are designed to perform at 4% air voids, actual field (construction) compaction typically results in mixtures in-place with an air void content in the range of  $7 \pm 1$  percent when opened to traffic. While secondary compaction under traffic will eventually reduce this air void content to approximately 4% over the course of three to five years, the occurrence of stripping is usually attributed to this early period in the life of the mixture, before the mixture “closes up.” Therefore, it was deemed realistic to compact samples

for the moisture susceptibility tests within the  $7 \pm 1$  percent range after two-hour short-term aging. This is similar to the requirements of AASHTO T-283.

Under the older Marshall-based protocol (AASHTO T-283), prior to fabricating samples for this test, it was necessary to prepare a number of samples at different compactive efforts in order to estimate the compactive effort necessary to bring a sample to a state of  $7 \pm 1$  percent air voids. However, under the Superpave system, the ability to obtain the full history of compaction during the initial design phase permits an easy and more certain estimate of the number of gyrations necessary to achieve the needed  $7 \pm 1$  percent air voids, thereby obviating the need to manufacture multiple trial samples.

### *Sample Pre-conditioning*

As discussed in the literature review, existing tests typically involve a step in which compacted samples are first vacuum saturated and then further conditioned in a saturated state by freezing and thawing or by some other means prior to some form of mechanical test. It should be recognized that these existing tests seek to condition the sample to a state representing field conditions favorable to stripping to apply a sequence of quasi-mechanical stresses in the conditioned samples (freeze-thaw, boiling, etc.) and to subsequently perform mechanical tests to measure the degree of damage induced in the samples by the conditioning process as compared to the same tests performed on unconditioned samples. In other words, the mechanical testing is performed a posteriori to the conditioning protocol, rather than being a component part of the process of inducing moisture-related damage in the samples.

Recalling that stripping is defined as “the separation of the asphalt coating from the aggregate in a compacted HMA mixture in the presence of water under the action of repeated traffic loading,” it was felt that in order to successfully replicate the mechanism of stripping in the laboratory, it would be necessary to perform the mechanical tests in a manner representing the effect of repeated traffic loading on a pavement on samples in a state (degree of saturation) typical of in situ conditions. In this manner, the concept of separate conditioning and testing becomes blurred, and the process becomes more “realistic” of actual conditions. Consequently, this section addressed the pre-conditioning of HMA samples in preparation for the true simulative testing that follows.

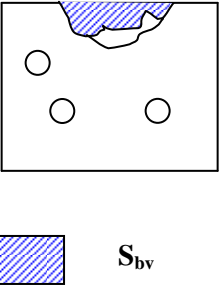
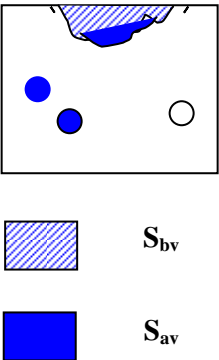
In the laboratory, it is difficult to control water penetration into HMA. Even though a number of methods are currently in use, it was decided to use the vacuum saturation method, which is used in national standard tests such as ASTM D1226 and AASHTO T 283. AASHTO T 283 requires that the samples be brought to 55%–80% saturation. However, it was felt that this procedure should be modified.

The current methods rely, at some point, on removal of the saturated sample from the saturating bath in order to determine the mass of the saturated and surface dry sample and ultimately to perform the required physical tests. This action, it is felt, permits the sample to drain and compromises the method. It was consequently decided that, having induced the appropriate degree of saturation in the sample, it should remain immersed in water throughout ensuing testing in order to more closely simulate real field pavement conditions.

The problem was raised how the degree of saturation could be measured without removing the vacuum saturated sample from the water in order to determine the mass of the saturated surface dry sample ( $W_{ssd}$ ), which is a subjective measure needed to calculate the degree of saturation under the current national standard test (ASTM D 2726). This problem was solved by using the automatic vacuum sealing method (Corelock™ device), recently selected as national standard test (ASTM D6752). A specimen of known dry mass is vacuum sealed in a specially fabricated plastic bag with the automatic vacuum chamber and then weighed in water. The  $G_{mb}$  for the specimen is calculated using these measurements. In this procedure, it is possible to calculate the  $G_{mb}$  without direct knowledge of the saturated and surface dry mass,  $W_{ssd}$ .

Based upon the information obtained from the automatic vacuum sealing methods ( $G_{mb}$ ,  $V_a$ ) and other available physical information obtained during the saturation process, a new calculation method for the degree of saturation is proposed. The method is outlined in Table 7.

**Table 7. The sequences of changes in asphalt mixture specimen with water and vacuum condition**

| Mix condition   | Illustration  | Definition  |
|---|---|---|
| <p>Before applying vacuum pressure</p> <p>Surface of mix absorbs water when mix is immersed in water; but not all surface accessible voids may be filled with water</p> |   | <p>- <math>G_{mb}</math> is defined as follows:<br/> <math display="block">G_{mb} = W_{dry} / (W_{ssd} - W_{sub})</math></p> <p>- Solving for <math>W_{dry}</math>, one obtains<br/> <math display="block">W_{ssd} = W_{dry} / G_{mb} + W_{sub}</math></p> <p>- Degree of saturation before applying vacuum:<br/> <math display="block">S_{bv} = \{ (W_{ssd} - W_{dry}) \times \gamma_w \} / V_a \times 100 \quad (1)</math></p> <p>where<br/> <math>W_{ssd}</math> = mass of surface dry specimen obtaining from equation<br/> <math>W_{dry}</math> = mass of specimen in air<br/> <math>V_a</math> = volume of air void<br/> <math>\gamma_w</math> = unit weight of water at room temperature</p> |
| <p>After vacuum</p> <p>Surface available air trapped in the mix is removed by applying vacuum, and water is absorbed into this area</p>                                 |  | <p>- Degree of saturation after applying vacuum:<br/> <math display="block">S_{av} = \{ (W_{cav} - W_{cbv}) \times \gamma_w \} / V_a \times 100 \quad (2)</math></p> <p>where<br/> <math>W_{cav}</math> = mass of the vacuum container adding water and specimen <i>after</i> vacuum<br/> <math>W_{cbv}</math> = mass of the vacuum container adding water and specimen <i>before</i> vacuum</p>  |

The total degree of saturation of specimens is then estimated as follows:

$$S_t = S_{bv} + S_{av} , \quad (3)$$

where

$S_t$  = Total saturation rate of mixture specimen in water and vacuum

$S_{bv}$  = Saturation rate of mixture specimen before applying vacuum pressure

$S_{av}$  = Saturation rate of mixture specimen after applying vacuum pressure

Water temperature during vacuum saturation was also considered to be important. Even though room temperature (25°C) is specified in current national standard tests, 35°C was selected for this project because it was believed by the Iowa DOT bituminous engineer and his staff that this temperature is more typical of conditions at the bottom of asphalt pavements in Iowa.

The relationship between the degree of saturation to be achieved and the time (duration) and magnitude of applied vacuum necessary to achieve that degree of saturation was also considered. Work by Tuncliff and Root (35) demonstrated that the degree of saturation at a fixed temperature was very sensitive to the magnitude of applied vacuum and practically independent of the time duration of the vacuum. This was confirmed by a trial and error process of changing the vacuum pressure and duration and monitoring the degree of saturation in samples having different void contents. In other words, increasing the magnitude of vacuum results in highly increased levels of saturation. However, even though increasing the duration of vacuum slightly affected the degree of saturation, this value remained essentially constant after a relatively short duration. Vacuum pressures of 10, 15, and 20 inHg were used to obtain the different degrees of saturation over specific durations of vacuum. Table 8 summarizes the test conditions in the proposed moisture pre-conditioning system.

**Table 8. Test conditions in the proposed moisture pre-conditioning system**

|                          |         |         |          |
|--------------------------|---------|---------|----------|
| Temperature              | 35°C    |         |          |
| Saturation Time (min)    | 1 – 5   |         |          |
| Vacuum Pressure (inHg)   | 10      | 15      | 20       |
| Degree of Saturation (%) | 50 – 65 | 65 – 80 | 80 – 100 |

#### Pre-conditioning Summary

- Samples are to be prepared using the Superpave Gyratory Compactor, bringing the samples to an air void content,  $V_a$ , in the range  $7\% \pm 1\%$ .
- Samples will be tested “dry” (i.e., unconditioned) and “saturated” (i.e., conditioned)
- Saturated samples will be vacuum saturated into three ranges of saturation ( $S_1=50\%–65\%$ ,  $S_2=65\%–80\%$  and  $S_3=80\%–100\%$ ).
- Saturated samples will remain submersed in water throughout the subsequent testing.

## *Evaluating Testing*

Under real conditions, water damage in asphalt pavement occurs only when the interior of the asphalt pavement is (partially) saturated and under the repeated traffic. It was felt that a repeated load should be applied to saturated and immersed samples to more closely reflect real conditions. Most current tests, except the wheel tracking tests, are performed under quasi-static loading conditions on saturated samples removed from the water, i.e., in a drained condition. It was decided to use the Nottingham Asphalt Tester (NAT) as an evaluation tool in this situation. NAT has the capability to perform a repeated dynamic load test.

The repeated load of the NAT was applied to saturated samples while immersed in water, at a constant temperature of 35°C. The load was repeated at a frequency of 0.5 Hz until sample failure. In this manner, the saturated sample is repeatedly loaded and water can be inhaled into and exhaled from the sample with each application of load. This allows a dynamic saturation condition, which is absent from other test methods.

### **Pilot Study**

Although the NAT is becoming the standard testing equipment throughout Europe, as far as it is known, this project represents the first attempt to use the NAT to evaluate moisture susceptibility in HMA mixtures. Therefore, to ensure the practicability of its use, a pilot test was first undertaken.

Using two aggregates (crushed limestone and crushed gravel), asphalt (PG 58-28), and two different gradations (coarse and dense), four different types of mixes (two aggregates by two gradation) were used in the pilot test. These samples were pre-saturated, as required before tested in the NAT. A temperature of 35°C was used in conjunction with a deviator stress of 230 kPa. The maximum test duration of the equipment, 10,000 cycles, was used to ensure that the critical failure condition would be captured. Each specimen was placed in NAT for approximately two hours before applying loading to ensure adequate and stable internal temperature. Due to the thermal inertia of the water used to immerse the samples, a “set” temperature of 38°C for two hours would bring the internal temperature of the sample to the required 35°C (47). The NAT records the sample permanent strain after each application of load and records the strain history of the sample throughout the duration of the test.

A complete discussion of the pilot test is provided in Kim (47). The information learned from the pilot test is summarized below:

1. Dry limestone mixtures deformed little during the full 10,000 applications of load and appeared to be in a stable (Stage II) mode.
2. Dry gravel mixtures demonstrated much higher rates of deformation than the corresponding limestone mixtures and clearly showed tertiary (Stage III) deformation.
3. The deformation histories of the dry samples compare the inherent differences between the two aggregate types in the absence of any stripping. This reflects the

- effect of the aggregate shape and texture on the mechanical strengths of the mixtures and demonstrates clearly why the amounts of uncrushed gravel particles are limited under DOT specifications when gravel mixtures are used.
4. It was observed that coarse-graded gravel mixtures were more sensitive to the degree of saturation than dense-graded gravel mixtures. This is in general agreement with field observation. It is believed that this is a reflection of the distribution and continuity of voids within the mixtures. While both sets of samples have essentially the same total void content, the voids in the dense-graded mixtures are probably discrete and not interconnected, while the voids in the coarse-graded mixtures are more likely to demonstrate a greater degree of interconnectivity, thereby allowing easier access to moisture and a greater likelihood of dynamic moisture flow within the mixtures.

Based on these conclusions, the main test protocol is described in the next section.

### **Final Laboratory Testing Protocol**

The main laboratory testing protocol followed the Superpave volumetric mix design method as described above, which allows for a moisture-sensitivity test to be performed on samples at the design binder content. Laboratory work can be broken down into five distinct steps, as shown below:

1. Volumetric mix design (Superpave)
2. Preparing samples—batching, mixing, aging, and compaction
3. Moisture pre-conditioning—sample saturation
4. Evaluating testing—NAT testing
5. Visual inspection

#### *Superpave Volumetric Mix Design*

Superpave volumetric mix design was performed to determine the optimum binder content for each aggregate blend. The procedures and criteria of Superpave volumetric mix design have been slightly modified since 1999, and this study adopted these modified procedures (41). After mixing, the loose mixture was aged for two hours at 135°C and 100 gyrations were applied to compact the mixture (this represents a traffic level of 3–30 million ESAL<sub>20</sub>).

Optimum binder contents were obtained for each mixture tested: this involved the determination of the binder content necessary to achieve 4% air voids, while simultaneously satisfying other volumetric criteria (VMA, VFA, Dust Proportion (DP), and Film Thickness (FT)). The optimum binder contents and other characteristics of the mixes used are listed in Table 9, and the terminologies used in volumetric mix design of HMA are described in Appendix A.

**Table 9. The result of Superpave mix design for each aggregate blend**

| TYPE  | P <sub>b</sub> | G <sub>mb</sub> | G <sub>mm</sub> | G <sub>se</sub> | P <sub>ba</sub> | P <sub>be</sub> | V <sub>a</sub><br>(=4.0)* | VMA<br>(>13)* | VFA<br>(65-75)* | DP<br>(0.6-1.6)* | FT<br>(8-13)* |
|-------|----------------|-----------------|-----------------|-----------------|-----------------|-----------------|---------------------------|---------------|-----------------|------------------|---------------|
| DLL   | 5.3            | 2.381           | 2.480           | 2.693           | 0.595           | 4.737           | 4                         | 15.0          | 73.3            | 1.1              | 8.5           |
| CLL   | 5.3            | 2.377           | 2.476           | 2.688           | 0.465           | 4.859           | 4                         | 15.2          | 73.7            | 1.0              | 9.9           |
| DGS   | 4.5            | 2.363           | 2.461           | 2.635           | 0.201           | 4.318           | 4                         | 13.9          | 71.3            | 0.9              | 8.7           |
| CGS   | 4.6            | 2.363           | 2.462           | 2.640           | 0.245           | 4.366           | 4                         | 14.0          | 71.5            | 1.1              | 8.9           |
| D5050 | 5.0            | 2.372           | 2.471           | 2.666           | 0.495           | 4.480           | 4                         | 14.3          | 72.1            | 0.9              | 9.0           |
| C5050 | 4.7            | 2.364           | 2.463           | 2.645           | 0.096           | 4.609           | 4                         | 14.6          | 72.4            | 1.1              | 9.4           |

\* Superpave volumetric mix design criteria.

### *Sample Preparation*

All of the coarse aggregates were washed before sieving. Washed coarse aggregates and fine aggregates were dried, sieved, and stored in five-gallon containers. These aggregate fractions were proportioned to make the aggregate blends: 4700 grams of blended aggregate were used for both coarse- and fine-graded aggregate blends, with 5% passing the ASTM #200 sieve (75 micron), and 4648 grams of blended aggregate were used for dense-graded aggregate blends, with 4% passing the ASTM #200 sieve.

Aggregate blends were heated in an oven overnight to 135°C before mixing. A temperature of 135°C was also used for mixing, short-term aging, and compaction temperatures in accordance with Iowa DOT specifications. The heated aggregates were placed into a heated mixing bowl and dry mixed by hand. The asphalt binder, which had been preheated to 135°C for approximately one and a half hours to be sufficiently fluid to pour, was added, and then the asphalt–aggregate mixture was mixed mechanically for 30–45 seconds and then mixed by hand until a uniform coating was observed. The resulting mix was aged for two hours in an oven at 135°C and was stirred after one hour to ensure uniform heating.

The samples were to be compacted to achieve 7% ± 1% air voids. This required a different number of gyrations for each mixture. These numbers were interpolated from the compaction curve obtained during the Superpave volumetric mix design for each mixture and were verified by measuring the bulk specific gravity of each sample and calculating the air voids after compaction and cooling. The number of gyrations required for each mixture is shown in Table 10.

The 48 mixtures were prepared in the laboratory. These mixtures have air void range from 6.8% to 7.6%, with standard deviation from 0.25 to 0.49. They were divided into two sets to be tested under the proposed test procedure with replication. The testing order was randomized in order to avoid any possible systematic error (47).

**Table 10. The number of gyration for different blended aggregates**

| Type of blended aggregates | Optimum Binder Content (%) | Number of Gyration | Average Air Void (%) | Standard Deviation |
|----------------------------|----------------------------|--------------------|----------------------|--------------------|
| CLL                        | 5.3                        | 47                 | 6.8                  | 0.37               |
| DLL                        | 5.3                        | 32                 | 7.6                  | 0.25               |
| C5050                      | 4.7                        | 39                 | 6.8                  | 0.36               |
| D5050                      | 5.0                        | 31                 | 7.1                  | 0.25               |
| CGS                        | 4.6                        | 29                 | 7.1                  | 0.37               |
| DGS                        | 4.5                        | 27                 | 6.9                  | 0.49               |

#### *Moisture Pre-conditioning—Saturating Samples*

Compacted mixes in each set were divided into two groups; one for dry (unconditioned) testing and the other for saturated testing. The dry group was tested in the NAT without moisture conditioning, and the saturated group was saturated as part of the moisture pre-conditioning protocol. Three levels of saturation were achieved by controlling the level and duration of the vacuum applied. Each specimen was immersed in a water bath at  $25^{\circ}\text{C} \pm 1^{\circ}\text{C}$  for  $4 \pm 1$  minutes, and the immersed mass ( $W_{\text{sub}}$ ) was recorded. The sample was transferred to the vacuum container without removing it from water. The lid was placed on the vacuum container and pressed gently. The vacuum container was then removed and placed on a flat desktop. Using a syringe, the container was gently filled with water until water flowed smoothly from the sides. Excess water was wiped from the container. The weight of the filled vacuum container with the sample ( $W_{\text{cbv}}$ ) was measured and combinations of vacuum and duration were applied to achieve the required degree of saturation. After completing the vacuum process, the vacuuming container was filled with water and the weight of vacuum container ( $W_{\text{cav}}$ ) was recorded. The degree of saturation was calculated using the suggested equations 1, 2, and 3. The results are provided in Appendix B.

#### *Evaluating Testing—NAT Testing*

The protocol of NAT testing was based on the results of pilot test. However, in the pilot test, a 230 kPa vertical stress was applied to the samples, but the results obtained were observed to have indicated sample failure related to material properties rather than to moisture damage. It was decided to reduce the magnitude of the applied load to 100 kPa, which is in agreement with the recommendations of European practice. Another factor that was addressed was the effect of the water pressure. In the testing of saturated specimens, the samples are surrounded by water, which provides a measure of confining stress, which is absent when testing samples in the dry. This difference was verified by testing “dry” samples with a membrane while submerged (47). However, it was difficult to quantify this effect because of equipment limitations. Consequently, in the main experiment, “dry” samples were tested in water, but protected from it by a rubber membrane—in this manner, the confining pressures on both sets of samples were at least approximately equalized.

As a result of these practical considerations, a final testing protocol (Table 11) was adopted.



**Table 11. NAT test condition used**

| <b>Test Property</b>     | <b>Test Condition</b>                              |
|--------------------------|--|
| Temperature              | 35°C—dry sample<br>38°C —saturated sample in water |
| Repeated vertical stress | 100 kPa  |
| Number of repetitions    | 10,000 cycles (5.5 hr)                             |
| Preconditioning time     | 2 hours at test temperature                        |

### **Summary**

The objective of this phase is to define a rigorous, realistic, usable laboratory testing protocol based on Superpave mix procedures. This laboratory testing protocol was based on observations made from results obtained during pilot testing.

Samples were fabricated at  $7\% \pm 1\%$  air void content by following Superpave volumetric mix procedures. These samples were randomly selected and divided into a dry conditioning group and a moisture conditioning group. The dry conditioning group was directly tested using the repeated load test in the NAT; however, these samples were tested in water, but sealed from the water by a membrane. The moisture conditioning group was pre-saturated at different degrees of saturation by vacuum conditioning and then tested in the NAT. The test conditions are summarized in Tables 8 and 11.

## **ANALYSIS OF TEST RESULTS AND DISCUSSION**

In this chapter, the results obtained from the designed laboratory tests are shown and analyzed. The final conclusions are developed and presented from the discussion of the results.

A number of factors need to be discussed prior to any analysis. While the mixtures tested met the design requirements for Superpave mixtures, there are distinct response differences between them due to textural differences between the aggregates. This will result in different responses to loading in the NAT, even between unconditioned or “dry” samples. This effect must not be confounded with the responses due to saturation. Consequently, results for each material combination must be normalized to its dry condition. Further, as will be reported, there was only limited visual evidence of stripping (of the binder from the aggregate), but it is clear that the presence of moisture in a mixture is detrimental to the behavior of asphalt mixtures and constitutes some form of moisture damage. Three analytical approaches (flow number, C- $\phi$  failure, and fracture energy) were applied to test data to determine the critical transition from sound to unsound for each tested mixture.

### **Laboratory Test Results**

NAT results were provided in Kim (47). These results report the percentage of accumulated permanent axial strain and the resilient modulus with increasing numbers of load repetition under each test condition. The slope, calculated at each point in the graph representing the percentage of accumulated permanent axial strain with the number of load repetitions, is also reported. The latter was necessary to discriminate between general material failure and moisture-related failure.

The percentage of accumulated permanent axial strain corresponding to the number of load repetitions is plotted in Figures 2 and 3. The curve is generally defined by the three zones: primary, secondary, and tertiary (42). The accumulated permanent strain rapidly increases in the primary zone due to sample compaction. The incremental permanent deformation decreases, reaching a more or less constant slope, and is stable in the secondary zone. In the tertiary zone, the incremental permanent deformation and the accumulated permanent axial strain again increase so that the number of load repetitions at the initiation of the tertiary zone is generally identified with the total accumulation of traffic necessary to cause permanent deformation failure (rutting). In this study, the percentage of accumulated permanent axial strain curve in the gravel mixtures and the 50/50 mixtures showed three distinct zones, but the limestone mixtures did not show the tertiary zone (i.e., more than 10,000 cycles would be needed to cause failure in the limestone mixtures).

From even a cursory examination of the results (Figure 2 and Figure 3) it is clear that the presence of moisture to some extent compromises the mixtures tested. The difficulty lies in identifying a method of analysis that adequately captures the relative degree of damage caused.

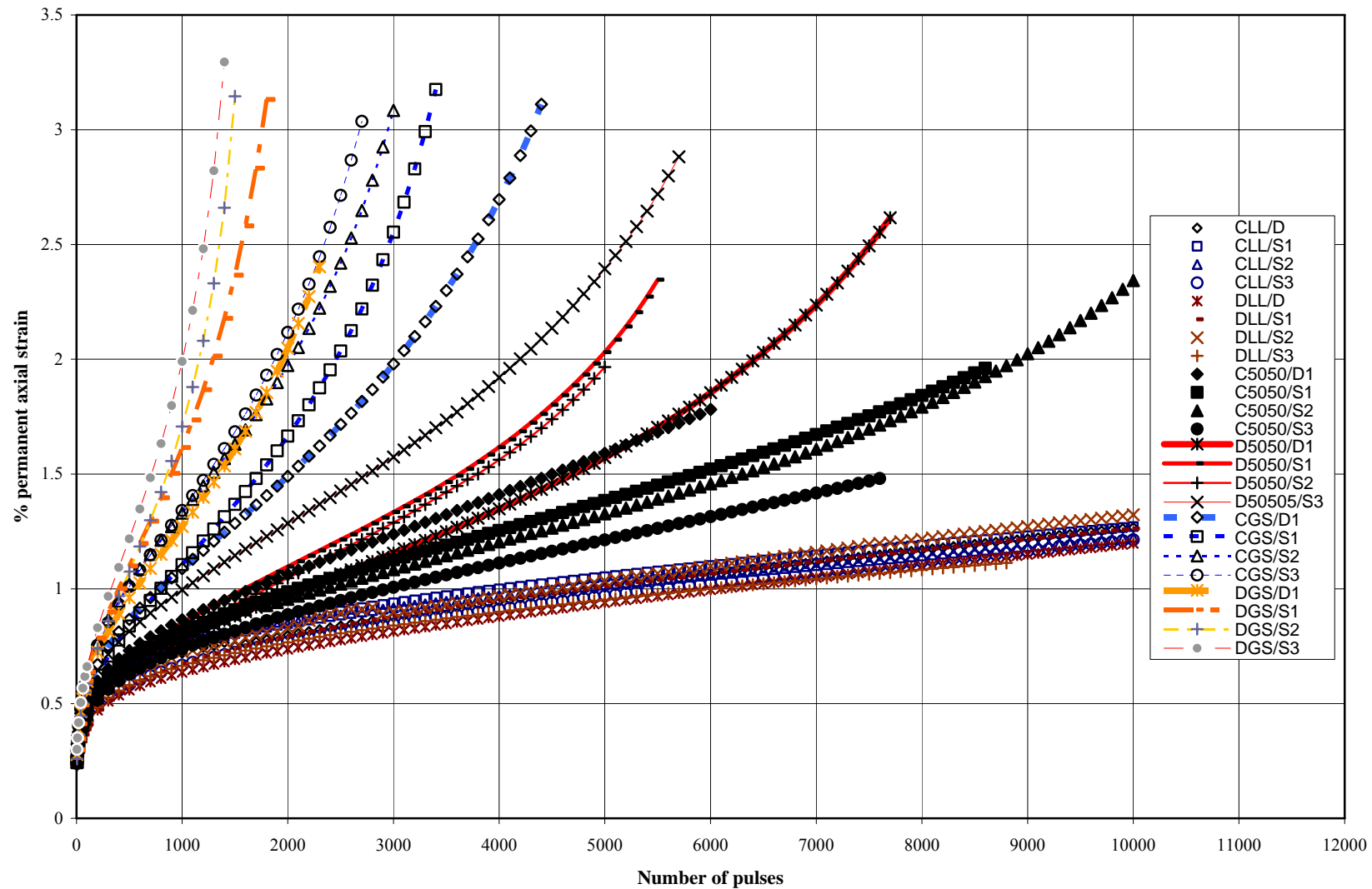
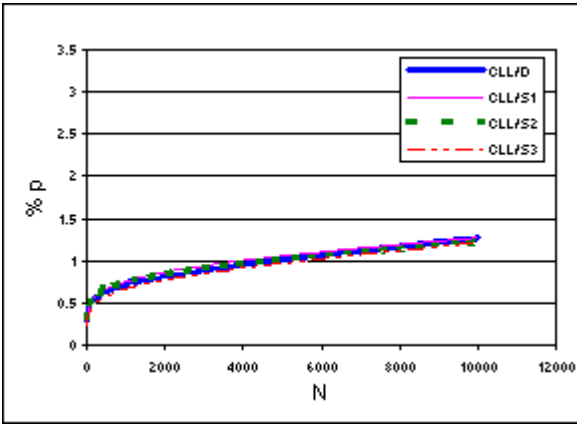
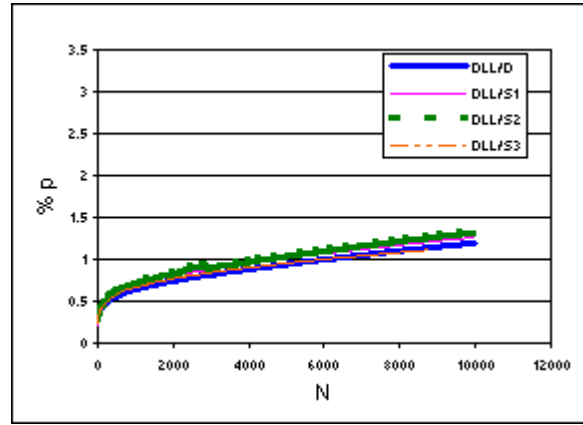


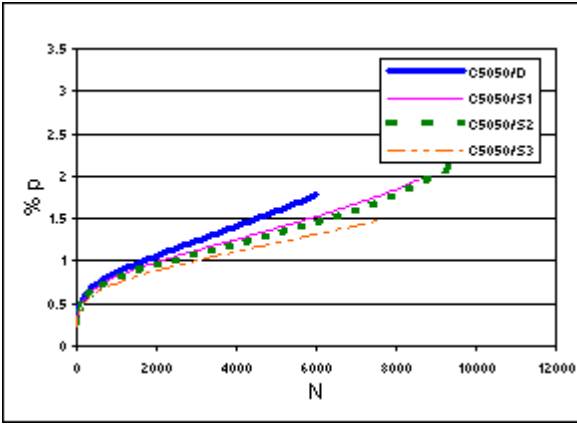
Figure 2. Summary of percentage of accumulated permanent axial strain in repeated load test with NAT



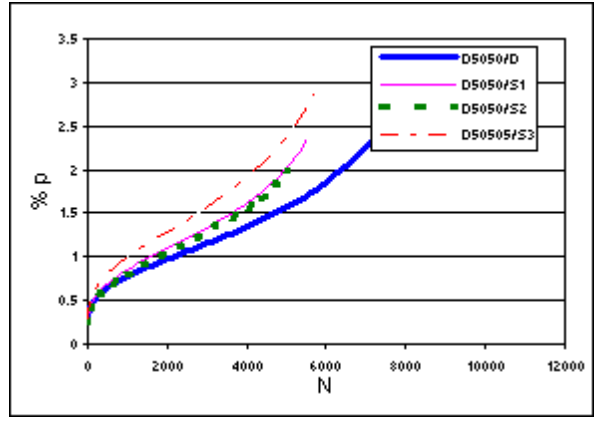
(a) CLL



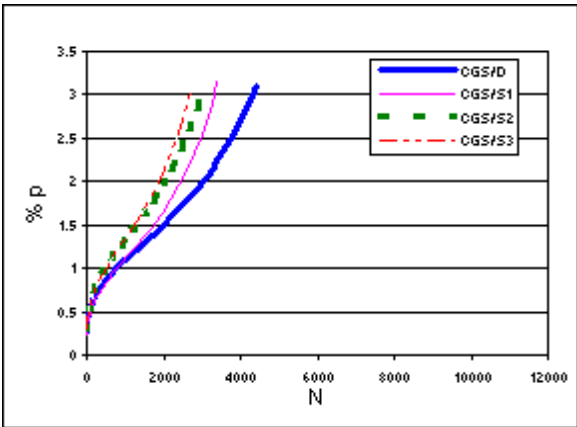
(b) DLL



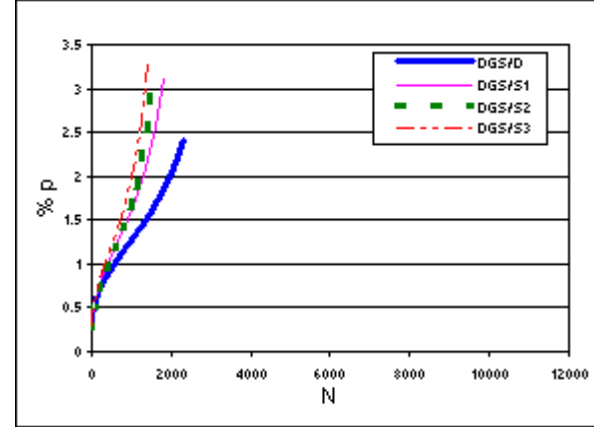
(c) C50/50



(e) D50/50



(f) CGS



(g) DGS

Figure 3. Percentage of accumulated permanent axial strain for each mixture

## Analysis of NAT Data

The analysis of test data focused on which response in the repeated load test results would best define the condition at which the mixture would be transformed from sound to unsound (i.e., a failure condition) and what were the differences between unconditioned and conditioned specimens at these failure points. Three analytical approaches were considered. Kaloush et al. (42) proposed the concept of the flow number to identify a critical state of HMA mixtures, i.e., the state at which mixtures transition from stable secondary zone to unstable tertiary zone. Kim (47) suggested that the raw data results indicate the occurrence of Cohesion and Friction failures (C-failure and  $\phi$ -failure) within samples and combined this observation with the flow number concept. Finally, Birgisson et al. (45) applied the principles of fracture mechanics to stripping and proposed the use of the Dissipated Creep Strain Energy (DCSE) and the Fracture energy (FE). This approach, with modification was used. The analyses of the data from this project were examined using each of these approaches.

Visual observation of the exposed fractured faces of tested specimens and statistical analysis followed these steps in order to identify which analytical approaches indeed reflected HMA moisture sensitivity.

### *Analytical Approach*

#### The Flow Number Approach

Kaloush et al. (42) proposed that the flow number, i.e., that number of load repetitions at which a sample transitions from stable (secondary zone) to unstable (tertiary one), should provide a good measure related to the performance of a mixture.

It was necessary to calculate the incremental permanent axial strain at each cycle in order to find the starting point of the tertiary zone. The slope of the permanent axial strain versus the number of load repetitions is plotted in Figures 4 and 5. The number of load repetitions corresponding to the point of inflection (minimum) of these curves is defined as the flow number and is considered to represent the starting point of the tertiary zone. These flow numbers representing critical permanent deformation failure in the gravel and the 50/50 mixtures can be observed on the curves. The ratio of the flow number of critical permanent deformation failure between the moisture conditioned and unconditioned specimens ( $RFN_p$ ) for the gravel and the 50/50 mixtures was calculated by Equation 4.

$$RFN_p = FN_p \text{ of Conditioned Specimen} / FN_p \text{ of Unconditioned Specimen} \quad (4)$$

where

$RFN_p$  = Retained flow number depending on critical permanent deformation failure

$FN_p$  = Flow number of critical permanent deformation failure

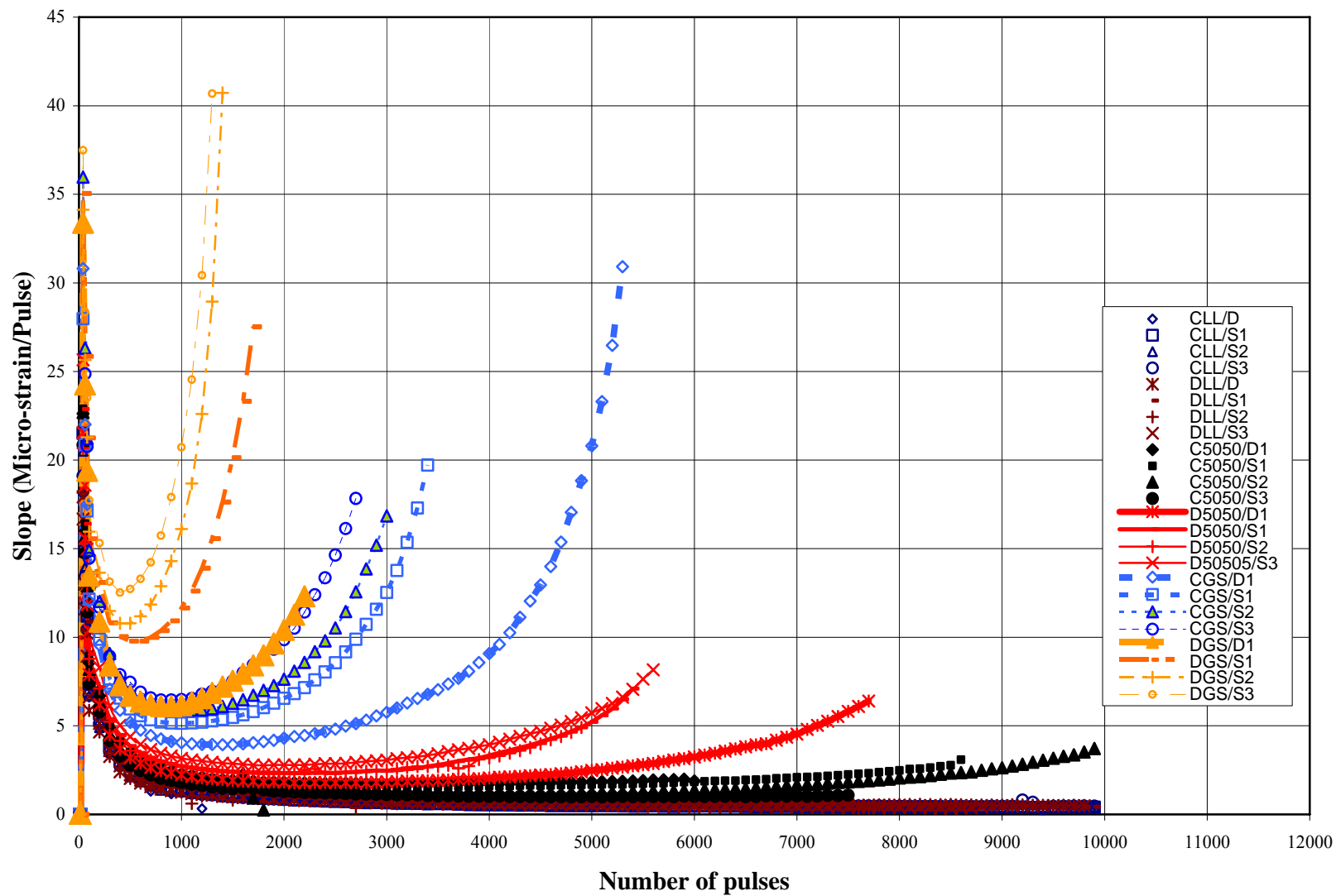
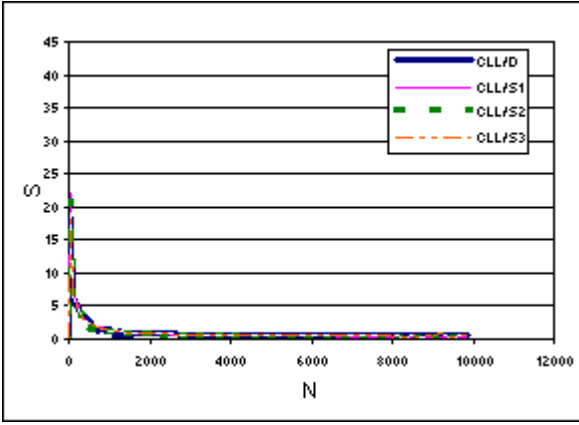
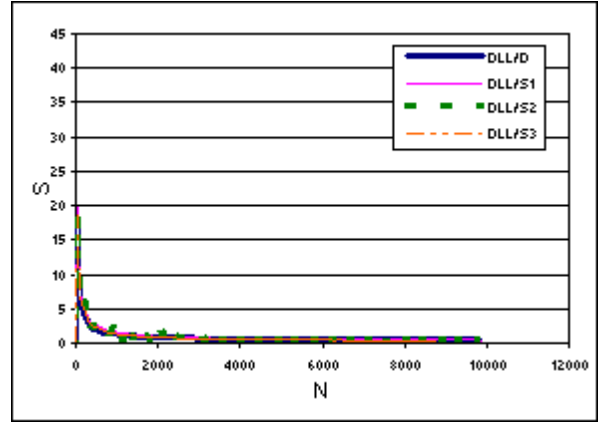


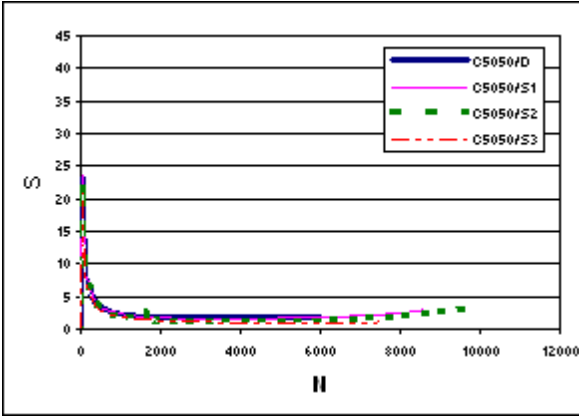
Figure 4. Slope of the permanent axial strain in repeated load axial test with NAT



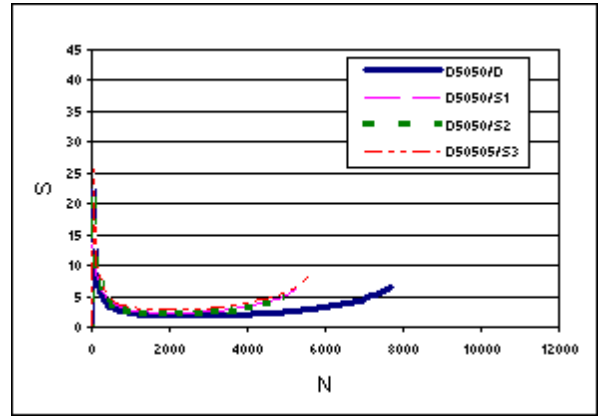
(a) CLL



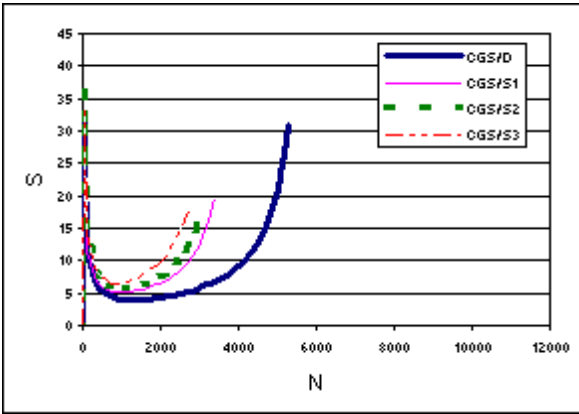
(b) DLL



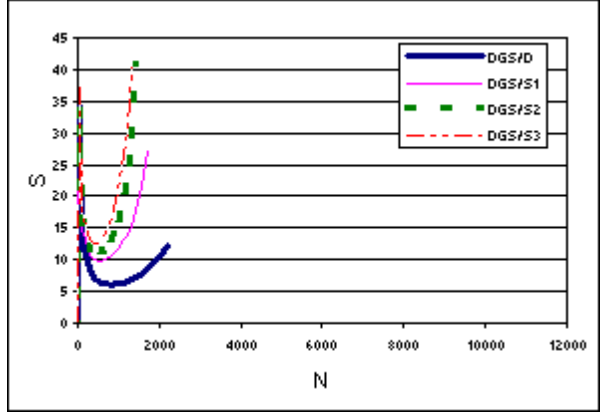
(c) C50/50



(e) D50/50



(f) CGS



(g) DGS

Figure 5. Slope of the permanent axial strain for each mixture

The RFN<sub>p</sub> for the gravel and the 50/50 mixtures is also shown in Figure 6 and is used to evaluate the moisture sensitivity. The RFN<sub>p</sub> for the gravel mixtures showed a significant difference since gravel is known to be a moisture sensitive aggregate. However, the RFN<sub>p</sub> for the gravel mixtures did not show much difference between the degrees of saturation, and, for the 50/50 mixtures, was greater than 100% at some degrees of saturation. It is hypothesized that there may be some pore water pressure built up during the repeated load test in moisture conditioned specimens. This residual pore water pressure made the specimen more elastic and resistant to permanent deformation. Allen and Deen reported a similar observation in a study to develop a rutting model with a repeated loading test in dense-graded aggregates (43). However, water also provides a lubricating effect during the tests so that permanent deformation failure developed more readily in the more water sensitive aggregate–gravel mixtures. This indicates that a criterion based on permanent deformation alone is not sufficient, but leads to an interesting discussion on how the effect of the pore water pressure and the lubricating effect of water in the mix can be separated.

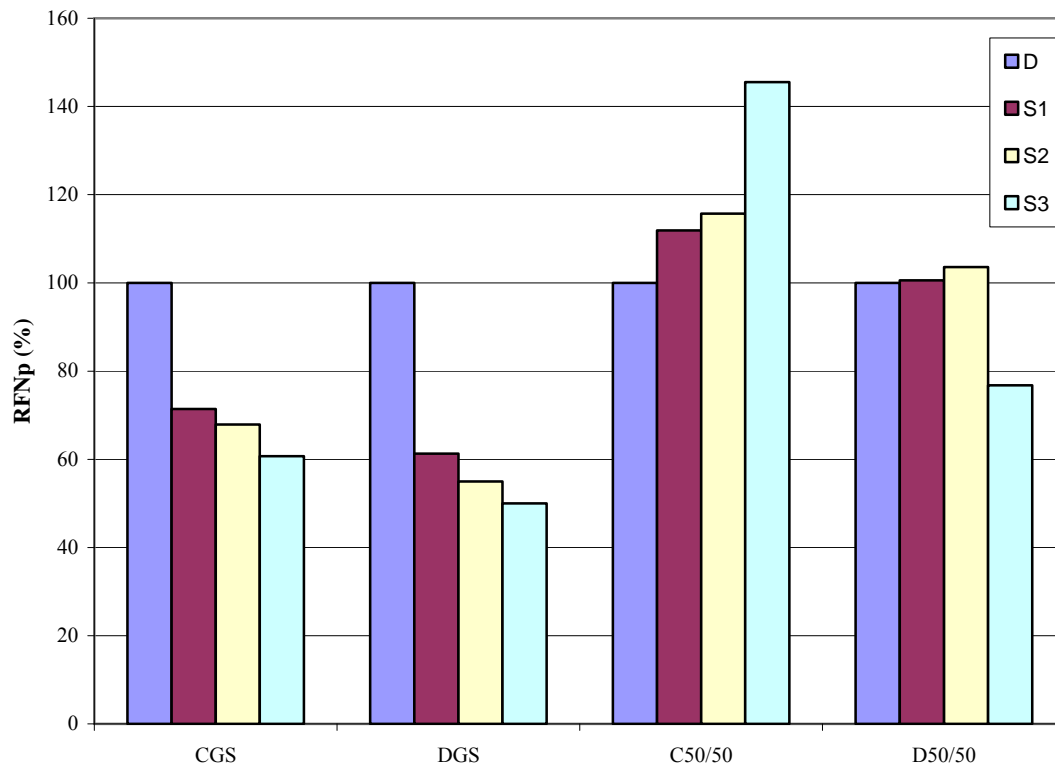


**Figure 6. RFN<sub>p</sub> for unconditioned and moisture conditioned mixtures**

#### Cohesion–Friction Failure Analysis

It is very difficult to measure the pore water pressure during the tests because of the limitations of the equipment setup. Consequently, it was proposed to analyze the resilient modulus versus the number of load repetitions because, like the current tests, this analysis should be based on strength failure rather than on permanent deformation failure. Resilient modulus versus the



number of load repetitions for each mixture was provided in Kim (47). As may be observed, the resilient modulus ( $M_r$ ) in the limestone mixtures increased up to a certain point and then became essentially constant. The interesting relationships between the resilient modulus and number of repetitions occurred in the other mixtures. In these mixtures, especially the gravel mixtures in Figure 7, a dramatic decrease in resilient modulus between successive points could be observed. It appears that the first point of loss of modulus might be related to cohesion failure and the second point to friction failure. Cohesion failure reflects the cohesive failure of the asphalt binder and may include stripping between the asphalt binder and the aggregate. However, cohesion failure in the dry samples can only reflect load-associated failure, not moisture-related cohesion failure. The difference between the dry and conditioned results, therefore, should only reflect the effect of moisture-related cohesion failure. Friction failure is the failure of the internal friction in aggregates. Apparently, the presence of moisture damage in HMA resulted in cohesion failure. Even though the numbers of load repetitions between two points between two test sets were different, the shape of these curves was the same. The ratio of the number of load repetitions at corresponding cohesive failure in conditioned specimens to that in the unconditioned specimens ( $RFN_C$ ) for gravel mixtures and 50/50 mixtures was calculated by Equation 5.

$$RFN_C = FN_C \text{ of Conditioned Specimen} / FN_C \text{ of Unconditioned Specimen} \quad (5)$$

where

$RFN_C$  = Retained flow number depending on cohesion failure

$FN_C$  = Flow number corresponding cohesion failure

The  $RFN_C$  results are shown in Figure 8. As can be observed in Figure 8, the effect of the degree of saturation on the  $RFN_C$  for the gravel mixtures and the dense-graded mixtures is indicated by a successive reduction with increasing saturation. The reduced  $RFN_C$  for gravel was expected, but, for dense-graded mixture, this was not expected because the most of water damage in the HMA is typically (visually) observed in mixtures with coarse-graded aggregates. This seems to be related to the vacuum saturation process. It is hypothesized that while the coarse- and dense-graded mixtures both had approximately 7% air voids, the distribution of the voids with the two types of mixtures is different: the voids in the coarse-graded mixtures are larger and more likely to be interconnected, while in the fine-graded mixtures, the voids are smaller, more widely dispersed, and have less connectivity. This could lead to a damaging condition during vacuum saturation, where by forcing a degree of saturation on dense-graded samples, the only way to get the water into the internally unconnected voids requires rupturing the binder or mastic films between voids. This issue is addressed later.

Even though the analysis based on  $FN_P$  and  $FN_C$  has been shown to yield a difference for moisture sensitivity in different mixes, it has the potential to be misleading. In the process of evaluating the  $FN_P$  and  $FN_C$ ,  $FN_P$  is the number of load repetitions corresponding to the point of inflection of the curve representing the slope of the permanent axial strain to the number of pulses. The point of inflection is identified at the smallest value of the slope. However, frequently there is no unique value, but a plateau of smallest values over a range of load repetitions. If the  $FN_P$  of the unconditioned specimen is not selected properly, then the computed  $RFN_P$  becomes less precise. This problem also occurs in determination of  $FN_C$  where the  $FN_C$  is

determined by visual inspection of the graph. A better method of locating a plateau of the smallest values of the slope is necessary before criteria for evaluation of HMA moisture sensitivity can be confidently proposed.

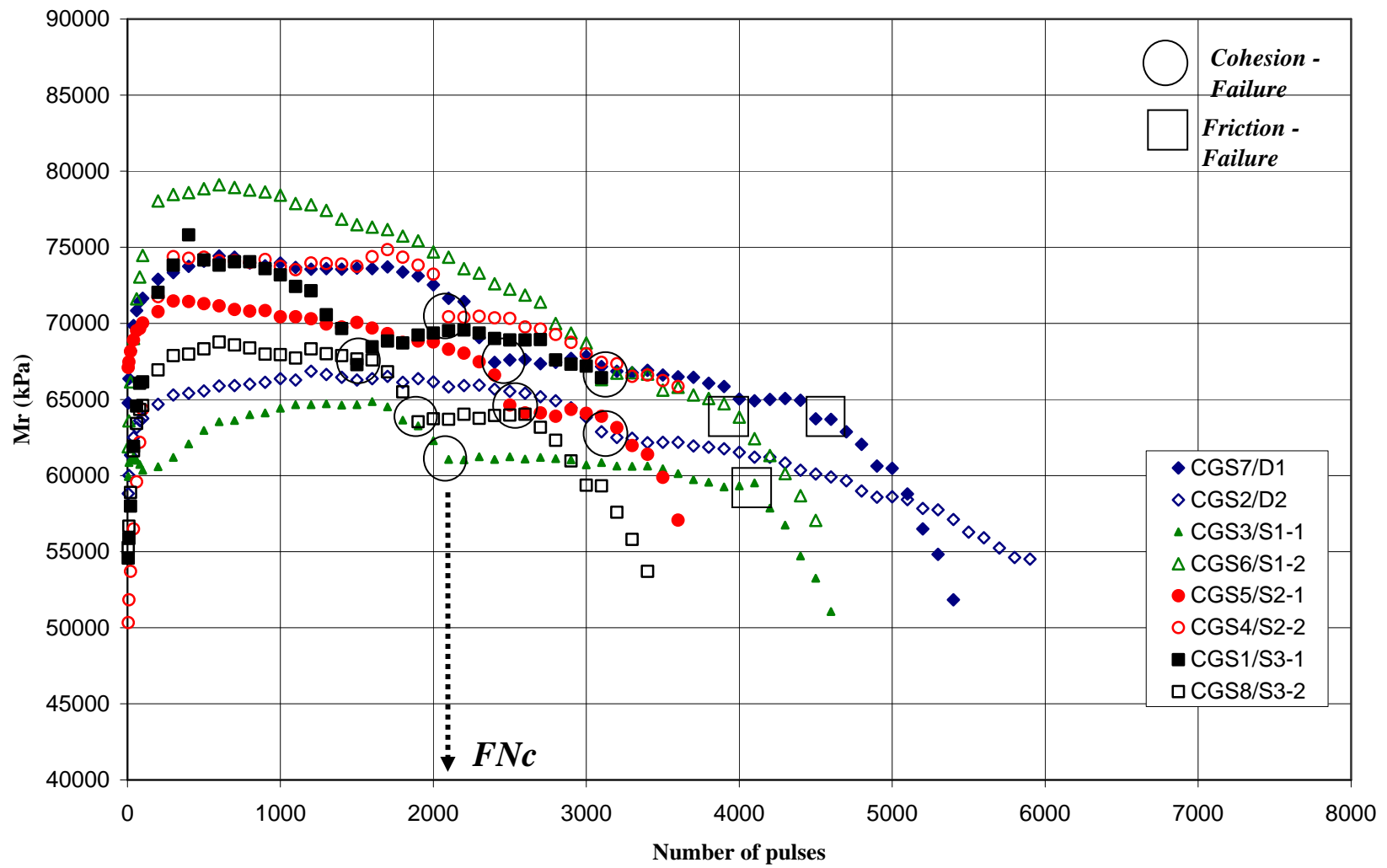
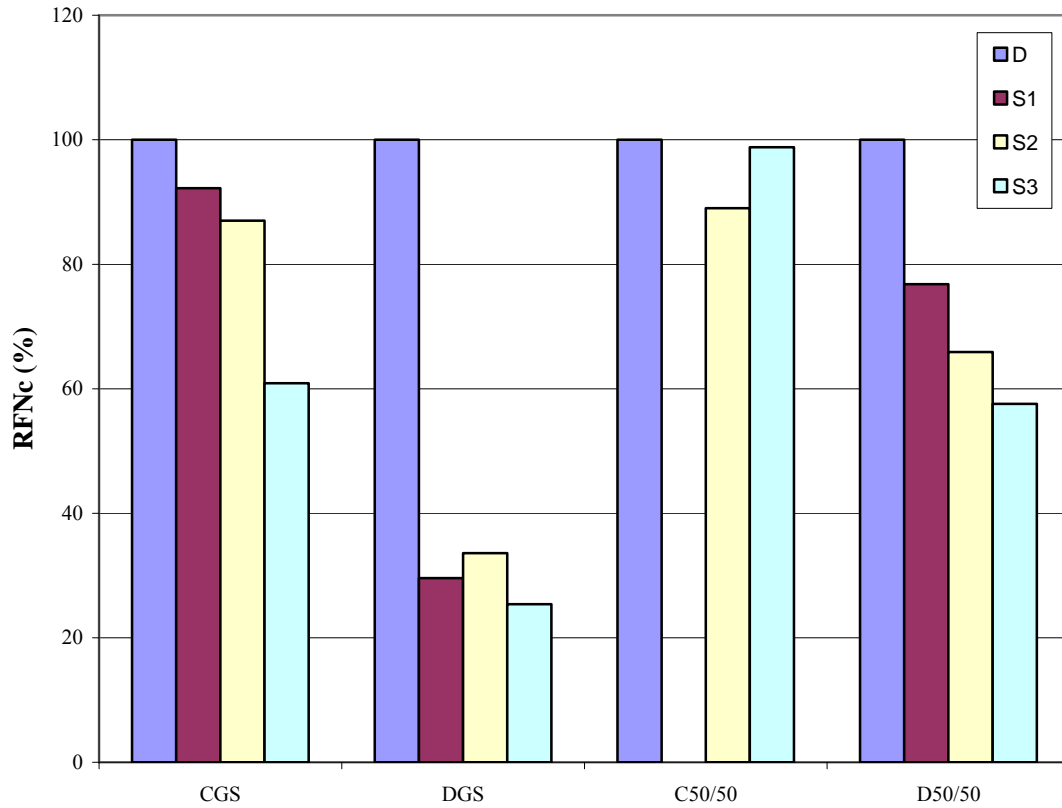


Figure 7. Resilient modulus in repeated load test for CGS with NAT



**Figure 8. RFN<sub>C</sub> for unconditioned and moisture conditioned mixture**

### Fracture Energy Approach

The analysis method based on fracture energy was suggested to avoid this problem. Roque et al. (44) showed that fracture energy (FE) of HMA is divided into dissipated creep strain energy (DCSE) and elastic energy (EE). They also suggested that the DCSE limit and the FE limit of HMA define the threshold of cracking behavior in HMA. Birgisson et al. (45) proposed an HMA fracture mechanics-based performance criterion, termed the energy ratio (ER), for quantifying the effect of moisture damage of HMA. energy ratio (ER) is defined as the ratio of dissipated creep strain energy at failure (DSCE<sub>f</sub>) with moisture damage to the minimum dissipated creep strain energy (DSCE<sub>min</sub>) for adequate cracking performance without moisture damage.

Even though this concept was applied to the results of repeated loading tests in the NAT, the equation for each term was modified since the Birgisson terms were based on the results of testing mixtures in tension, whereas herein the mixtures were tested in repeated compression to obtain a compression resilient modulus. The FE of HMA was divided into dissipated permanent strain energy (DPSE) (not dissipated creep strain energy [DCSE]) and elastic energy (EE) because the type of load in the proposed test was repeated loading, not static (creep) loading. DPSE and EE can be expressed by Equations 6 and 7.

$$DPSE \text{ (kJ/m}^3\text{)} = \int_0^N \frac{(\sigma \text{ max} + \sigma \text{ min})}{2} \Delta \varepsilon_p dN = \frac{\sigma \text{ max}}{2} \varepsilon_{P @ N} \quad (6)$$

where

$\sigma \text{ max}$  = Maximum load in each number of load pulse (kPa)

$\sigma \text{ min}$  = Minimum load in each number of load pulse (kPa) = 0

$\Delta \varepsilon_p$  = Permanent strain increments in each number of load pulse (m/m)

$\varepsilon_{P @ N}$  = Accumulated permanent strain at specific number of load pulse (m/m)

$$EE \text{ (kJ/m}^3\text{)} = \int_0^N \frac{(\sigma \text{ max} + \sigma \text{ min})}{2} \varepsilon_E dN = \frac{\sigma \text{ max}}{2} \int_0^N \frac{\sigma \text{ max}}{Mr} dN \quad (7)$$

where

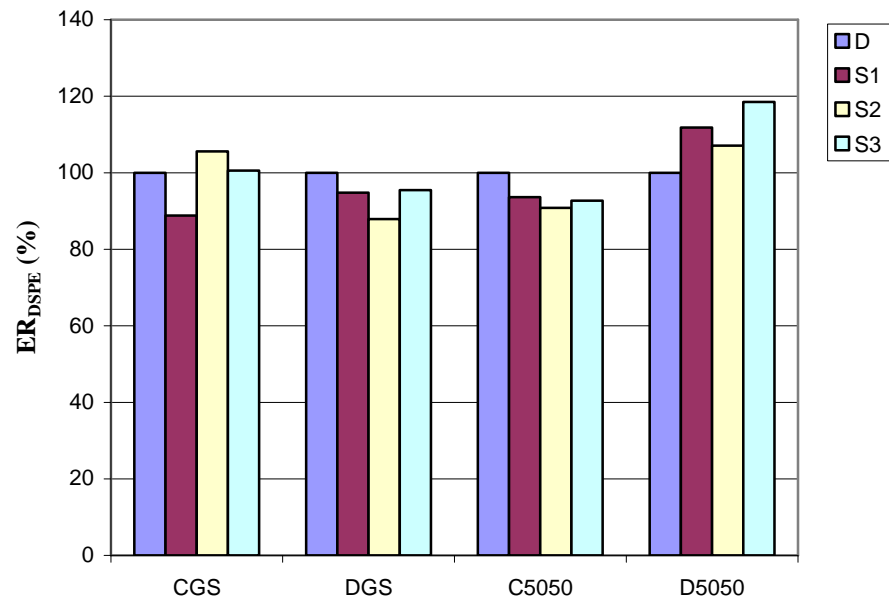
$\sigma \text{ max}$  = Maximum load in each number of load pulse (kPa)

$\sigma \text{ min}$  = Minimum load in each number of load pulse (kPa) = 0

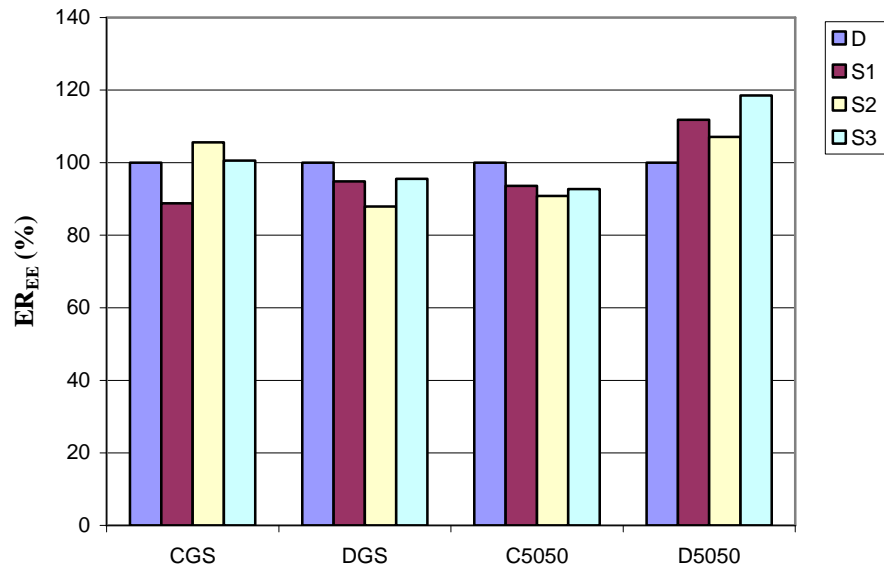
$\varepsilon_E$  = Elastic strain in each number of load pulse (m/m)

$Mr$  = Resilient modulus in each number of load pulse (kPa)

The terminology ER was modified to  $ER_{DPSE}$ , the ratio of the dissipated permanent strain energy in conditioned specimens to the dissipated permanent strain energy in unconditioned specimens, and to  $ER_{EE}$ , the ratio of the elastic strain energy in conditioned specimens to the elastic strain energy in unconditioned specimens. Figure 9 shows  $ER_{DSPE}$  and  $ER_{EE}$  at  $FN_p$  for each mixture, and Figure 10 shows  $ER_{DSPE}$  and  $ER_{EE}$  at  $FN_c$  for each mixture.

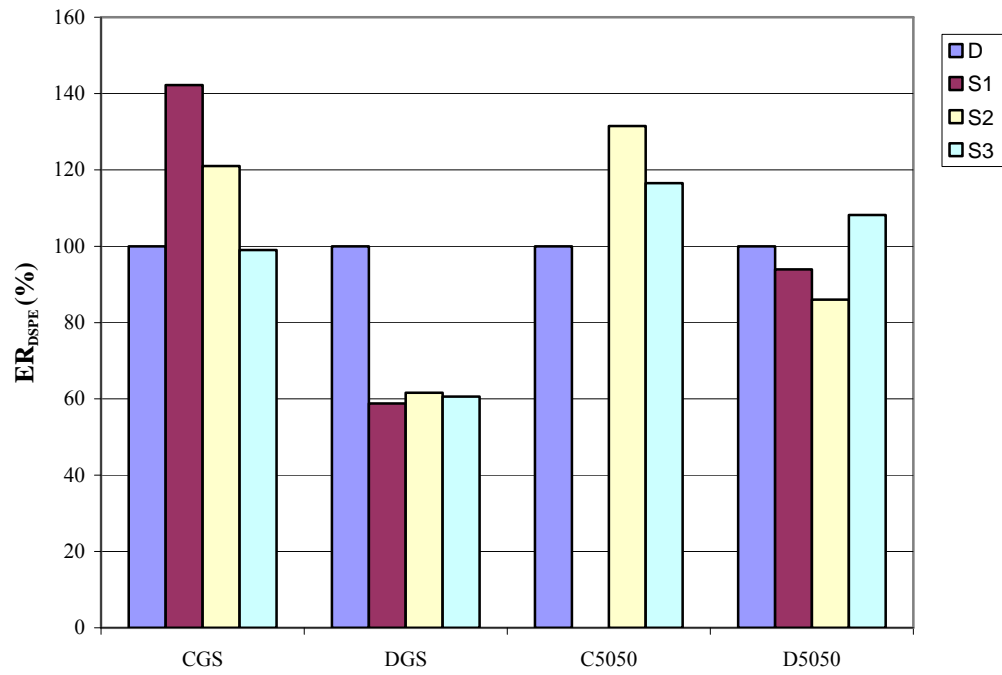


(a)  $ER_{DSPE}$  at  $FN_P$  for unconditioned and moisture conditioned mixtures

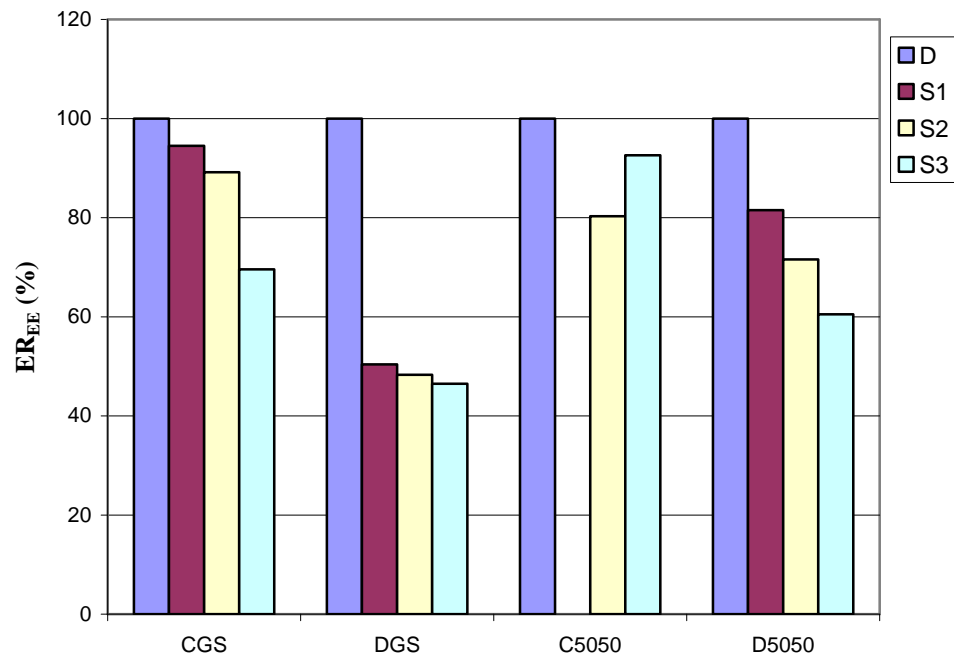


(b)  $ER_{EE}$  at  $FN_P$  for unconditioned and moisture conditioned mixtures

Figure 9. ER at  $FN_P$  for unconditioned and moisture conditioned mixtures



(a)  $ER_{DSPE}$  at  $FN_C$  for unconditioned and moisture conditioned mixtures



(b)  $ER_{EE}$  at  $FN_C$  for unconditioned and moisture conditioned mixtures

Figure 10. ER at  $FN_C$  for unconditioned and moisture conditioned mixtures

The comparison of  $ER_{DSPE}$  and  $ER_{EE}$  at  $FN_P$  and  $FN_C$  for unconditioned and moisture conditioned mixtures led to interesting discussions.

First,  $ER_{DSPE}$  and  $ER_{EE}$  at  $FN_P$  did not demonstrate much difference between unconditioned and moisture conditioned mixtures for gravel and 50/50 mixtures. In fact, there was a slight increase in  $ER_{DSPE}$  and  $ER_{EE}$  in the 50/50 mixtures. It indicates that  $ER_{DSPE}$  and  $ER_{EE}$  at  $FN_P$  do not have a clear criterion to evaluate the moisture damage of HMA.

Second, there are different values for  $ER_{DSPE}$  and  $ER_{EE}$  at  $FN_C$  for the different gradations and aggregate types. For DGS mixtures,  $ER_{DSPE}$  and  $ER_{EE}$  at  $FN_C$  decreased in moisture conditioned mixtures. However, the effect of the degree of saturation was insignificant. It is believed that these mixtures were damaged during the vacuum saturation phase before testing so that they rapidly fractured under load. It can be supported by the case for CGS, which can represent the fracture behavior due to only repeated loading system. For CGS mixtures,  $ER_{DSPE}$  increased and  $ER_{EE}$  decreased in moisture conditioned mixtures as the degree of saturation increased. Coarse-graded mixtures have more permeable void space than dense-graded mixtures and are less subject to damage under vacuum saturation.

### *Visual Observation*

Visual observation is needed to verify that the analysis in the previous section correctly identifies moisture damage in HMA. Notwithstanding this subjective approach, visual observation of a fractured specimen is a helpful method to check moisture-related adhesion failure. Stripping of aggregate was not evident in most of the samples inspected. It is believed that these specimen failures arose from cohesion failure rather than adhesive stripping failure. This general observation supports the hypothesis that the analysis based on  $FN_C$  can identify cohesion failure.

### *Statistical Analysis*

Statistical analyses—the analysis of variance (ANOVA) and the least significant difference (LSD)—were undertaken in each suggested parameter obtained from three analytical approaches for different type of blends with different treatments (Dry, S1, S2, and S3). In original plan, the comparison of full mixture combinations (CLL, DLL, C50/50, D50/50, CGS, and DGS) was expected. However, the limestone mixtures (CLL and DLL) did not show failure in the given number of load repetition (10, 000 cycles), and some data of C50/50 mixture for  $FN_C$  were not collected because the NAT did not reach 10,000 cycles. Thus, the data of limestone mixture were excluded from statistical analysis for all parameters, and the data of C50/50 were excluded from statistical analysis for some parameters associated with  $FN_C$  ( $RFN_C$ ,  $ER_{DSPE}$  at  $FN_C$ , and  $ER_{EE}$  at  $FN_C$ ).

ANOVA can provide information for the difference and the factor effects between aggregate combinations and degrees of saturation, but can not provide information between degrees of saturation within a single aggregate blend. LSD was undertaken to evaluate the differences in



degrees of saturation for a single aggregate blend. The results of statistical analysis are summarized in Table 12 from the complete results of statistical analysis in Kim (47).

From the Table 12, it can be drawn that  $RF_{Np}$ ,  $RF_C$ , and  $ER_{EE}$  at  $FN_C$  among suggested parameters provided a statistical difference in different mixture combinations with 95% confidence level, and there was difference between dry and different saturation levels, but no difference within different saturation levels.

**Table 12. Summary of statistical analysis for suggested parameters**

| Parameter           | Comparison     | F-Ratio | P-Value  | Effecting source*   | LSD*                                  |
|---------------------|----------------|---------|----------|---|---------------------------------------|
| $RF_{Np}$           | Gravel & 50/50 | 7.162   | 0.0002** | Type of aggregate<br>Type of gradation<br>Degree of saturation x Type of aggregate    | A***: Dry, S1, S2<br>B***: S1, S2, S3 |
| $RF_{Nc}$           | DGS & CGS      | 16.063  | 0.0004** | Degree of saturation<br>Type of gradation<br>Degree of saturation x Type of gradation | A : Dry<br>B : S1, S2, S3             |
|                     | DGS & D50/50   | 5.563   | 0.0137** | Degree of saturation<br>Type of aggregate   | A : Dry<br>B : S1, S2, S3             |
| $ER_{DSPE}$ @ $FNp$ | Gravel & 50/50 | 1.141   | 0.3971   | Type of aggregate x Type of gradation   | No difference                         |
| $ER_{EE}$ @ $FNp$   | Gravel & 50/50 | 3.633   | 0.0073** | Degree of saturation<br>Type of aggregate<br>Degree of saturation & Type of aggregate | No difference                         |
| $ER_{DSPE}$ @ $FNc$ | DGS & CGS      | 8.973   | 0.003**  | Type of gradation<br>Degree of saturation x Type of gradation                         | A: Dry<br>B: S1, S2, S3               |
|                     | DGS & D50/50   | 0.859   | 0.5730   | None  | No difference                         |
| $ER_{EE}$ @ $FNc$   | DGS & CGS      | 7.119   | 0.0064** | Degree of saturation<br>Type of gradation   | A : Dry<br>B : S1, S2, S3             |
|                     | DGS & D50/50   | 6.512   | 0.0085** | Degree of saturation<br>Type of aggregate<br>Degree of saturation & Type of aggregate | A : Dry<br>B : S1, S2, S3             |

\* 95% confidence. \*\* Significantly different at 95% confidence

\*\*\* There is no significant difference in same letter.

## Summary

The objective of this chapter was to discuss the laboratory test results and to analyze the results using different approaches to suggest the criteria for the evaluation of HMA moisture sensitivity using proposed test protocol.

The result of proposed test procedure is provided in Kim (47). There are three different approaches to analysis these results.

One is based on permanent deformation failure. The flow number corresponding to the critical permanent deformation ( $FN_P$ ) for each mix was obtained (Figure 4), and the retained flow number depending on critical permanent deformation failure ( $RFN_P$ ) for each mix was calculated with Equation 4.  $RFN_P$  for each mix is plotted in Figure 6.

The analysis based on cohesive failure is suggested. The flow number corresponding to cohesion failure ( $FN_C$ ) for each mix was obtained from the plot of resilient modulus ( $Mr$ ) versus the number of repetitive loads (Figure 7). The retained flow number depending on cohesion failure for each mix ( $RFN_C$ ) could be also calculated with Equation 5.

The analysis based on the fracture energy is also considered because of the potential errors inherent in identifying a pessimum slope in the measurement of  $RFN_P$  and  $RFN_C$ . Fracture energy in HMA is divided into two phases—a dissipated permanent strain energy (DPSE) and elastic energy (EE). DPSE was calculated with Equation 6 and EE with Equation 7.  $ER_{DPSE}$  is defined as the ratio of the dissipated permanent strain energy in the conditioned specimen to the dissipated permanent strain energy in the unconditioned specimen, and  $ER_{EE}$  is defined as the ratio of the elastic strain energy in conditioned specimen to the elastic strain energy in unconditioned specimen. These fracture energy parameters at  $FN_P$  are plotted in Figure 9. The fracture energy parameters at  $FN_C$  are plotted in Figure 10.

Statistical analysis for suggested parameters was conducted and summarized in Table 12.  $RFN_P$ ,  $RFN_C$ , and  $ER_{EE}$  at  $FN_C$  identify a statistical significance of different mixtures and are affected by most factors that induce the moisture damage to HMA at 95% confidence. The other ER at  $FN_P$  or at  $FN_C$  is not statistically different for different mixtures. It also shows that there was difference between dry and different saturation levels, but no difference within different saturation levels.

It is important to recommend criteria for the evaluation of HMA moisture sensitivity based on the analyses undertaken. In spite of the results of statistical analysis, the analysis based on the permanent deformation failure ( $RNF_P$ ) appears to be influenced by pore water in the HMA (i.e., the permanent deformation is resisted by the pore water pressure). The analysis based on the elastic failure— $RNF_C$  and  $ER_{EE}$  at  $FN_C$ —has potential whether the failure of HMA arises from moisture damage of HMA or not. However,  $RNF_C$  analysis can be misleading due to the difficulty of estimating a clear value of  $RNF_C$ . It is also suggested that the vacuum saturation process used in this study may damage samples before the repeated loading test in NAT. That may be the reason why dense-graded mixes show more damage than coarse-graded mixes in this study.

## **General Discussion on the Air Void Distribution in HMA**

The method of moisture pre-conditioning samples is an important part in the proposed test. Vacuum saturation was used in the proposed test because it has been generally used in national standard tests—AASHTO T 283 and ASTM D4867. However, as previously mentioned, there are indications that vacuum saturation may rupture the internal structure of specimens even in the absence of external loading.

Air void distribution in HMA can be divided into two components. One component is the air void that is permeable to (external) water at atmospheric pressure ( $V_P$ ) (i.e., open to the outside of the sample), and the other component is the air void that is not permeable to water at atmospheric pressure ( $V_{NP}$ ) (i.e., closed to the outside of the sample).  $V_P$  is also divided into two parts—air void that can be saturated in saturated surface dry condition ( $V_{S@SSD}$ ) and air void that cannot be saturated in the saturated surface dry condition ( $V_{NS@SSD}$ ). In other words, when a sample is immersed in water, the externally available voids ( $V_P$ ) do not fully fill with water. There is usually some unsaturated surface void space remaining, trapped within the void structure, that can only be filled under vacuum pressure. Figure 11 shows this distribution in HMA.

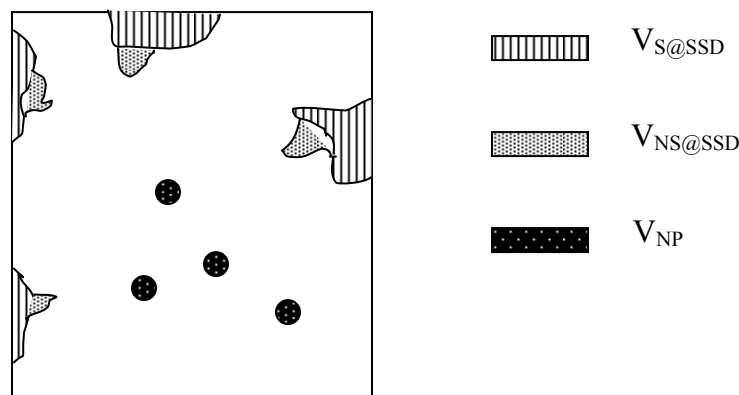


**Figure 11. Air void distribution in HMA**

The air content test by pressure method (ASTM C231), which is normally used to measure the air content in fresh concrete, was used to measure the unfilled surface available voids in samples. The air meter applies a small pressure to the HMA while submersed in water so that surface permeable voids are filled with water ( $V_{S@SSD}$  and  $V_{NS@SSD}$ ). The measured air content indicates the air content in the air meter container. Water in the air meter container is air free and incompressible so that this value can be used to calculate the volume of the entrapped air void ( $V_{NP}$ ) in HMA. This recalculated value indicates  $V_{NP}$  in terms of the percentage of air void. Samples representing the two different types of gradation—coarse and dense—were fabricated and tested following ASTM C231. Table 13 shows the results of this test.

**Table 13.  $V_{NP}$  of coarse and dense-graded mixture**

| Specimen ID | Air Voids, $V_a$ (%) | Indicated Air content (%) | $V_{NP}$ (%) | $V_{NP} / V_a$ (%) |
|-------------|----------------------|---------------------------|--------------|--------------------|
| CL 1        | 6.5                  | 0.8                       | 4.0          | 61.9               |
| CL 2        | 6.7                  | 0.7                       | 4.4          | 65.0               |
| AVG         | 6.6                  | 0.8                       | 4.2          | 63.4               |
| DL 1        | 6.0                  | 0.4                       | 4.7          | 78.7               |
| DL 2        | 6.6                  | 0.5                       | 5.0          | 76.1               |
| AVG         | 6.3                  | 0.5                       | 4.9          | 77.4               |

As indicated in Table 13, dense-graded mixes have larger values of impermeable voids ( $V_{NP}$ ) than coarse-graded mixes. The corollary is that the void space in coarse-graded mixes is more interconnected and externally open, while dense-graded mixtures contain more discrete voids, unconnected to the outside. The last column in Table 13 can be transformed by subtraction from 100; this gives the percentage of total air voids that are connected to the outside of the sample. For the dense mixtures tested, this averages 23%, and for the coarse mixtures, 37%. These figures also represent the limit to which these samples can be vacuum saturated without inducing structural changes. Since AASHTO T283 requires a minimum vacuum saturation of 55%, which value exceeds both of these figures, it is likely that the process of vacuum saturation, itself, damages the samples.

The value of  $V_{S@SSD}$  in HMA can be calculated with the Equation 8.

$$V_{S@SSD} = (W_{SSD} - W_{DRY}) / (W_{DRY} / G_{mb}) \quad (8)$$

where

$$\begin{aligned} W_{SSD} &= \text{Weight of mixture in surface saturated condition (g)} \\ &= W_{DRY} / G_{mb} + W_{SUB} \\ W_{DRY} &= \text{Weight of mixture in dry condition (g)} \\ W_{SUB} &= \text{Weight of mixture in submerged condition (g)} \\ G_{mb} &= \text{Bulk specific gravity of mixture} \end{aligned}$$

$W_{SUB}$  is recorded until the weight becomes constant. The value of  $V_{NP}$  is calculated with Equation 9.

$$V_{NP} = V_a - V_{S@SSD} - V_{NS@SSD} \quad (9)$$

where

$$\begin{aligned} V_a &= \text{Air void content in mixture (\%)} \\ V_{NP} &= \text{The content of air void that cannot be permeable with water at atmospheric pressure (\%)} \\ V_{S@SSD} &= \text{The content of air void that can be saturated in saturated surface dry condition (\%)} \\ V_{NS@SSD} &= \text{The content of air void that cannot be saturated in saturated surface dry condition (\%)} \end{aligned}$$

## CONCLUSIONS AND RECOMMENDATIONS

### Conclusions

HMA moisture damage mechanisms and tests that have been suggested were reviewed. An HMA moisture sensitivity testing protocol using the NAT was developed. The laboratory protocol was developed by focusing on inducing mechanical failure due to the moisture damage of HMA. The test data were analyzed with three different approaches: Retained flow number of critical permanent deformation ( $RFN_p$ ), retained flow number of cohesion failure ( $RFN_c$ ), and energy ratio (ER).

Based on the literature review, laboratory test, and analysis of test data, the following conclusions were made.

#### *Literature Review*

1. Moisture damage of HMA can be defined as the separation between asphalt and aggregate and the weakness of attractive force between asphalt and aggregate resulting from moisture and field traffic action.
2. Moisture damage of HMA is influenced by various factors, such as aggregate properties, asphalt properties, type of mixture, environmental effects during/after construction, and agents or modifiers (5).
3. The mechanism of moisture damage in HMA has been developed from emphasizing the fundamental aspect of attractive forces between asphalt and aggregate through connecting this with real traffic situations (26, 27).
4. Many suggested tests have provided various simulations based on many mechanisms of moisture damage of HMA and supplemented these with a visual inspection and a physical value related to performance (5).
5. Even though various concepts and test protocols of moisture damage of HMA have been suggested, the conclusion of these concepts and test results cannot explain all observed cases of moisture damage in HMA pavements.

#### *Laboratory Test*

1. The proposed laboratory testing can eliminate handling and transferring the specimen from water bath to testing device, which is a possible source of error.
2. The proposed laboratory testing uses the repeated loads to simulate traffic movement on pavement.
3. The proposed laboratory testing can rapidly assess potential of moisture damage for HMA (1 day) without the freezing and thawing procedure, which makes the current national test procedure take longer time (7 days).
4. The proposed laboratory testing is divided into three phases: specimen preparation (compaction), moisture pre-conditioning, and evaluating test.
5. Specimen preparation follows the specification of Superpave volumetric mix design. Samples are compacted to an air void content of  $7\% \pm 1\%$  (sample height = 117 –

- 118 mm).
6. Even though vacuum pressure saturation was used in proposed test, it is hypothesized that vacuum saturation may in itself damage the samples.
  7. It could be noted that the use of crushed limestone as a filler ( $P_{200}$ ) was not providing an anti-strip function.
  8. High vertical stresses (230 kPa) in NAT may cause mechanical rather than moisture-related failure in samples.
  9. The effect of water pressure surrounding saturated test specimens is not a negligible factor.

### *Analysis of Test Data*

1. The results for each mixture must relate the conditioned test results to the dry test results due to textural differences between the aggregates.
2. The effect of moisture can be clearly observed from a cursory examination of the data. The difficulty lies in identifying a method of analysis that adequately captures the relative degree of damage.
3. The proposed test method provided a number of analysis parameters from the tested specimen (e.g., RFN based on permanent deformation failure, RFN based on cohesion failure,  $ER_{DPSE}$  and  $ER_{EE}$  at  $FN_P$ , and  $ER_{DPSE}$  and  $ER_{EE}$  at  $FN_C$ ).
4. The difference between the dry test and conditioned test results for cohesion failure should only reflect the effect of moisture.
5.  $RFN_C$  and  $RFN_P$  provided a statistical difference in different types of mixes with 95% confidence. However, analyses based on  $RFN_C$  and  $RFN_P$  may be uncertain due to the difficulties in separating the resistant effect of pore water pressure and the lubricating effect of water.
6.  $ER_{DSPE}$  and  $ER_{EE}$  at  $FN_P$  do not indicate a clear criterion to evaluate the moisture damage of HMA.
7.  $ER_{EE}$  at  $FN_C$  provided a statistical difference between the different mixtures at 95% confidence.
8. The statistical difference between the dry and the different saturation level mixtures could be identified. However, there was no statistical difference within different saturation level mixtures.
9. The stripping of aggregate was not clearly evident by visual inspection. It appears that the failure of specimen therefore derives from a cohesive failure of binder, not binder stripping failure from aggregate.
10. Air void distribution in HMA can be separated into two components—the air voids that are not accessible to water at atmospheric pressure ( $V_{NP}$ ) and the air voids that are water-permeable at atmospheric pressure ( $V_P$ ).  $V_P$  is further divided into two portions—air voids in  $V_P$  that can be saturated in saturated surface dry condition ( $V_{S@SSD}$ ) and air voids in  $V_P$  that cannot be saturated in saturated surface dry condition ( $V_{NS@SSD}$ ). This is demonstrated through the results of air content test by pressure method (ASTM C231). This conclusion proposes that the vacuum pressure saturation carries a risk of damaging the internal structure of HMA.
11. As indicated in Table 13, the void space in coarse-graded mixtures is more interconnected and externally open, while dense-graded mixtures contain more discrete void.

## Summary

From the literature review, laboratory testing, and analysis of the data collected, even though the proposed laboratory testing can more closely and rapidly replicate the effect of repeated traffic loading on in situ conditioned HMA than current national standard test, it is clear that quantifying HMA moisture sensitivity is not easy to explain and is difficult to measure.

The HMA moisture sensitivity should be some parameter which can represent the relative reduction of physical properties between unconditioned (dry) and conditioned (wet) HMA.

Analysis based on  $ER_{EE}$  at  $FN_C$  shows a higher potential for evaluating HMA moisture sensitivity than other methods examined. The currently specified degrees of vacuum saturation are not appropriate.

## Recommendations

The literature review, laboratory test, and analysis of data in this study have suggested the following recommendations:

1. Validate the test procedure with real mixes and compare with the current national standard test (AASHTO T283) to establish specification limit.
2. Develop a database of tests on field-cored specimens so that a stronger analysis may be conducted to validate the correlation between laboratory-fabricated specimens and field-cored specimens.
3. Evaluate the effect of anti-stripping agents through the proposed laboratory testing.
4. Review the procedure for vacuum saturation used in AASHTO T283 and the proposed test in order to avoid damaging samples during this process.

## REFERENCES

1. Hubbard, P. "Adhesion of Asphalt to Aggregate in Presence of Water." *Proceedings of the Highway Research Board*, Vol. 8, Part 1, 1938.
2. Kiggundu, B.M. and Roberts, F.L. *Stripping in HMA Mixtures: State of The Art and Critical Review of Test Methods*. NCAT Report 88-2, National Center for Asphalt Technology, September 1988.
3. Kandhal, P.S. *Moisture Susceptibility of HMA Mixes: Identification of Problem and Recommended Solutions*. NCAT Report 92-1, National Center for Asphalt Technology, May 1992.
4. Stuart, K.D. *Moisture Damage in Asphalt Mixtures – A State of the Art Report*. FHWA-RD-90-019, Federal Highway Administration, August 1990.
5. Hicks, R.G. "Moisture Damage in Asphalt Concrete." *NCHRP Synthesis of Highway Practice*, Vol.175, Transportation Research Board, October 1991.
6. Majidzadeh, K. and Brovold, F. N. *Effect of Water on Bitumen – Aggregate Mixtures – State of the Art*. Special HRB Report, No. 98, Highway Research Board, 1968.
7. Kennedy, T.W., Roberts, F.L., and LEE, K.W. "Evaluation of Moisture Susceptibility of Asphalt Mixtures Using the Texas Freeze-Thaw Pedestal Test." *Proceedings of the Association of Asphalt Paving Technologists*, Vol. 53, 1982.
8. Tunnicliff, D.G. and Root, R.E. "Antistripping Additives in Asphalt Concrete – State of the Art 1981." *Proceedings of the Association of Asphalt Paving Technologists*, Vol. 53, 1982.
9. Lee, A.R. and Nicholas, J.W. "Adhesion in Construction and Maintenance of Roads." *Adhesion and Adhesives, Fundamentals and Practice*, Society of Chemical Industry, London, 1954.
10. Rice, J.M. "Relationship of Aggregate Characteristics to the Effect of Water on Bituminous Paving Mixtures." *ASTM STP 240*, American Society for Testing and Materials, 1958.
11. Barksdale, R.D. *The Aggregate Handbook*. National Stone Association, Washington, D.C., 1991.
12. Povarennykh, A.S. *Crystal Chemical Classification of Mineral*. Plenum Press, New York –London, 1972.
13. Sanderson, F.C. "Methylchlorosilanes as Antistripping Agent." *Proceedings of the Highway Research Board*, Vol.31, 1952.
14. Mark, C. "Physic-Chemical Aspects of Asphalt Pavements: Energy Relations at Interface between Asphalt and Mineral Aggregate and Their Measurement." *Industrial and Engineering Chemistry*, 1935.
15. Hubbard, P. "Adhesion in Bituminous Road Materials: A Survey of Present Knowledge." *Journal of the Institute of Petroleum*, Vol. 44, No. 420, pp.423-432, 1958.
16. Bikerman, J.J. "The Rheology of Adhesion." *Rheology, Theory and Application*, Vol.3, 1960.
17. Kanitpong, K. and Bahia, H. U. "Role of Adhesion and Thin Film Tackiness of Asphalt Binders in Moisture Damage of HMA." *Proceedings of the Association of Asphalt Paving Technologists*, Vol. 72, 2002.
18. Terrel, R.L. and Al-Swailmi, S. *Water Sensitivity of Asphalt – Aggregate Mixes: Test Selection*. Report SHRP-A-403, Strategic Highway Research Program, National Research Council, Washington, D.C., 1994.



19. Thelen, E. "Surface Energy and Adhesion Properties in Asphalt-Aggregate System." *Proceeding of the Highway Research Board*, Bulletin 192, 1958.
20. Kim, Ok-Kee., Bell, C.A. and Hicks, R.G. "The Effect of Moisture on the Performance of Asphalt Mixtures." *ASTM STP 899*, American Society for Testing and Materials, 1985.
21. Schmidt, R.J. and Graf, P.E. "The Effect of Water on the Resilient Modulus of Asphalt Treated Mixes." *Proceedings of the Association of Asphalt Paving Technologists*, Vol.41, 1958.
22. Curtis, C.W., Terrel, R.L., Perry, L.M., AL-Swailm, S., and Braanan, C.J. "Importance of Asphalt –Aggregate Interactions in Adhesion." *Proceedings of the Association of Asphalt Paving Technologists*, Vol. 60, 1991.
23. Terrel, R.L., and Shute, J.W. *Summary Report on Water Sensitivity*. SHRP-A/IR-89-003, Strategic Highway Research Program, National Research Council, 1989.
24. Brown, A.B., Sparks, W.J., and Marsh, E.G., "Objective Appraisal of Stripping of Asphalt from Aggregate." *ASTM STP 240*, American Society for Testing and Materials, 1985.
25. Takallou, H.T., Hicks, R.G., and Wilson, J.L., "Evaluation of Stripping Problems in Oregon." *ASTM STP 899*, American Society for Testing and Materials, 1985.
26. Lottman, P. R. "Laboratory Test Method for Predicting Moisture – Induce Damage to Asphalt Concrete." *Transportation Research Record*, No.843, 1982.
27. Taylor, A.Mark. and Khosla, N.Paul. "Stripping of Asphalt Pavements: State of The art." *Transportation Research Record*, No.911, 1983.
28. Fromm, J.H. "The Mechanisms of Asphalt Stripping From Aggregate Surfaces." *Proceedings of the Association of Asphalt Paving Technologists*, Vol. 43, 1974.
29. Gzemski, G.F., McGlashan, W.D., and Dolch, L.W. "Thermodynamic Aspects of the Stripping Problem." *Highway Research Circular*, No. 78, 1968.
30. R.P.Lottman. *Predicting Moisture-Induced Damage to Asphalt Concrete*. NCHRP Report 192, Transportation Research Board, October 1978.
31. R.P.Lottman. *Predicting Moisture-Induced Damage to Asphalt Concrete – Field Evaluation*. NCHRP Report 246, Transportation Research Board, May 1982.
32. *ASTM-Road and Paving Material; Vehicle-Pavement Systems*. Annual Book of ASTM Standards, V4.03, 1998.
33. *AASHTO-Standard Specification for Transportation Materials and Method of Sampling and Testing*. Part 3 edition, 1997.
34. Schmidt, J.R. and Graf, E.P. "The Effect of Water on the Resilient Modulus of Asphalt Treated Mixes." *Proceedings of the Association of Asphalt Paving Technologists*, Vol.60, 1991.
35. Tunicliff, G. David and Root, E. Richard. *Use of Antistripping Addictives in Asphaltic Concrete Mixtures*. NCHRP Report 274, Transportation Research Board, October 1984.
36. Tunicliff, G. David and Root, E. Richard. *Use of Antistripping Addictives in Asphaltic Concrete Mixtures*. NCHRP Report 373, Transportation Research Board, October 1984.
37. Curtis, C.W., Ensley, K., and Epps, J. *Fundamental Properties of Asphalt – Aggregate Interactions Including Adhesion and Absorption*. Final Report SHRP A-003B, 1991.
38. Allen, L.Wendy and Terrel, L.Ronald. *Field Validation of Environmental Conditioning System*. SHRP- A-396, Strategic Highway Research Program, National Research Council, 1994.
39. Epps, A.John, Sebaly, E.Peter, Penaranda, Jorge and et al. *Compatibility of a Test for Moisture – Induced Damage with Superpave Volumetric Mix Design*. NCHRP-444, Transportation Research Board, 2000.

40. Richard, P.Izzo and Maghsound Tahmoressi “Use of the Hamburg Wheel – Tracking Device for Evaluating Moisture Susceptibility of Hot-Mix Asphalt.” *Transportation Research Record*, No. 1681, 1999.
41. *Superpave Asphalt Mixture Design*, Version 8, Federal Highway Administration, 2002.
42. Kalous, E.W. and Wiczack, W.M, “Tertiary Flow Characteristic of Asphalt Mixtures.” *Proceedings of the Association of Asphalt Paving Technologists*, Vol. 71, 2002.
43. Allen, L.D. and Deen, R.C. “Rutting Models for Asphaltic Concrete and Dense-Graded Aggregate from Repeated-Load Tests.” *Proceedings of the Association of Asphalt Paving Technologists*, Vol. 49, 1980.
44. Roque, R., Birgisson, B., Sangpetngam, B. and Zhang, Z. “Hot Mix Asphalt Fracture Mechanics: A Fundamental Crack Growth Law for Asphalt Mixtures.” *Proceedings of the Association of Asphalt Technologists*, Vol. 71, 2002.
45. Birgisson, B., Roque, R. and Page, C.G. “The Use of a Performance – Based Fracture Criterion of the Evaluation of Moisture Susceptibility in Hot Mix Asphalt.” *Transportation Research Record*, 2004-3431, 2004.
46. Brown, R.E., Kandhal, S.P., and Zhang, Jingna. *Performance Testing for Hot Mix Asphalt*. NCAT Report 01-05, National Center for Asphalt Technology, November 2001.
47. Kim, S.H. “Evaluation of Hot Mix Asphalt Moisture Sensitivity Using the Nottingham Asphalt Test equipment.” MS thesis, Iowa State University, 2004.

## **APPENDIX A: THE TERMINOLOGY OF SUPERPAVE VOLUMETRIC MIX DESIGN**

The definition of terminology used in Superpave volumetric mix design is given below:

Pb = asphalt binder content by total weight of mix (%)

Gmb = mixture bulk specific gravity

Gmm = theoretical maximum specific gravity of the mix

Gsb = aggregate bulk specific gravity

Gse = aggregate effective specific gravity

Pba = absorbed asphalt binder content by weight of aggregate (%)

Pbe = effective asphalt binder content by total weight of mix (%)

Va = air voids in compacted HMA (%)

VMA = voids in the mineral aggregate (%)

VFA = voids filled with asphalt binder (%)

DP = ratio of P200 material to effective asphalt binder content

FT = average film thickness (microns)

## **APPENDIX B: MOISTURE PRE-CONDITIONING SYSTEM RESULTS**

**Table B.1. Moisture pre-conditioning results for set 1 specimens**

| Specimen ID. | Vacuum pressure (in Hg) | Gmb   | Gmm   | Va (%) | Wmdry (g) | Wmsub (g) | Wmssd (g) | S <sub>1</sub> (%) | Wcbv (g) | Wcav (g) | Wcav - Wcbv (g) | S <sub>2</sub> (%) | S <sub>T</sub> (%) |
|--------------|-------------------------|-------|-------|--------|-----------|-----------|-----------|--------------------|----------|----------|-----------------|--------------------|--------------------|
| DLL 5        | 0                       | 2.292 | 2.48  | 7.6    |           |           |           |                    |          |          |                 |                    |                    |
| DLL 4        | 10                      | 2.301 | 2.48  | 7.2    | 4704.5    | 2692.5    | 4737      | 22                 | 10289    | 10334    | 45.2            | 31                 | 53                 |
| DLL 7        | 15                      | 2.293 | 2.48  | 7.5    | 4710.6    | 2693.8    | 4748.1    | 24                 | 10291    | 10363    | 72.3            | 47                 | 71                 |
| DLL 6        | 20                      | 2.293 | 2.48  | 7.5    | 4705.2    | 2690.5    | 4742.5    | 24                 | 10289    | 10393    | 104.3           | 67                 | 92                 |
| CLL 2        | 0                       | 2.302 | 2.476 | 7.0    |           |           |           |                    |          |          |                 |                    |                    |
| CLL 4        | 10                      | 2.31  | 2.476 | 6.7    | 4709      | 2706.3    | 4744.8    | 26                 | 10300    | 10332    | 32.2            | 24                 | 50                 |
| CLL 3        | 15                      | 2.318 | 2.476 | 6.4    | 4713.8    | 2714.1    | 4747.7    | 26                 | 10312    | 10367    | 54.2            | 42                 | 68                 |
| CLL 7        | 20                      | 2.312 | 2.476 | 6.6    | 4705.3    | 2708.4    | 4743.6    | 28                 | 10301    | 10374    | 72.3            | 54                 | 82                 |
| D5050 5      | 0                       | 2.291 | 2.469 | 7.2    |           |           |           |                    |          |          |                 |                    |                    |
| D5050 7      | 10                      | 2.288 | 2.469 | 7.3    | 4702.4    | 2682.4    | 4737.6    | 23                 | 10277    | 10326    | 48.8            | 32                 | 56                 |
| D5050 4      | 15                      | 2.286 | 2.469 | 7.4    | 4702.8    | 2679      | 4736.2    | 22                 | 10278    | 10357    | 78.6            | 52                 | 73                 |
| D5050 2      | 20                      | 2.288 | 2.469 | 7.3    | 4706.1    | 2684.4    | 4741.3    | 23                 | 10280    | 10371    | 90.8            | 60                 | 84                 |
| C5050 3      | 0                       | 2.298 | 2.463 | 6.7    |           |           |           |                    |          |          |                 |                    |                    |
| C5050 6      | 10                      | 2.277 | 2.463 | 7.6    | 4703.4    | 2693      | 4758.6    | 35                 | 10289    | 10334    | 45.1            | 29                 | 64                 |
| C5050 8      | 15                      | 2.294 | 2.463 | 6.9    | 4706.2    | 2700.8    | 4752.3    | 33                 | 10295    | 10353    | 57.9            | 41                 | 74                 |
| C5050 1      | 10                      | 2.299 | 2.463 | 6.7    | 4707      | 2701.6    | 4749      | 31                 | 10299    | 10377    | 78.5            | 58                 | 88                 |
| DGS 5        | 0                       | 2.285 | 2.461 | 7.2    |           |           |           |                    |          |          |                 |                    |                    |
| DGS 4        | 10                      | 2.293 | 2.461 | 6.8    | 4697.1    | 2673.5    | 4722      | 18                 | 10270    | 10316    | 46.1            | 33                 | 51                 |
| DGS 2        | 15                      | 2.308 | 2.461 | 6.2    | 4704.2    | 2692.2    | 4730.4    | 21                 | 10287    | 10347    | 59.6            | 47                 | 68                 |
| DGS 1        | 20                      | 2.302 | 2.461 | 6.5    | 4703.3    | 2688      | 4731.1    | 21                 | 10286    | 10378    | 91.6            | 69                 | 90                 |
| CGS 7        | 0                       | 2.294 | 2.462 | 6.8    |           |           |           |                    |          |          |                 |                    |                    |
| CGS 3        | 20                      | 2.298 | 2.462 | 6.7    | 4708.5    | 2691.8    | 4740.8    | 24                 | 10287    | 10334    | 47.7            | 35                 | 59                 |
| CGS 5        | 15                      | 2.294 | 2.462 | 6.8    | 4707.3    | 2686.7    | 4738.7    | 22                 | 10284    | 10353    | 69.2            | 49                 | 72                 |
| CGS 1        | 20                      | 2.293 | 2.462 | 6.9    | 4703.4    | 2696.3    | 4747.5    | 31                 | 10291    | 10386    | 94.5            | 67                 | 98                 |

**Table B.2. Moisture pre-conditioning results for set 2 specimens**

| Specimen ID. | Vacuum pressure (in Hg) | G <sub>mb</sub> | mm    | V <sub>a</sub> (%) | W <sub>mdry</sub> (g) | W <sub>msub</sub> (g) | W <sub>mssd</sub> (g) | S <sub>1</sub> (%) | W <sub>cbv</sub> (g) | W <sub>cav</sub> (g) | W <sub>cav</sub> - W <sub>cbv</sub> (g) | S <sub>2</sub> (%) | S <sub>T</sub> (%) |
|--------------|-------------------------|-----------------|-------|--------------------|-----------------------|-----------------------|-----------------------|--------------------|----------------------|----------------------|---|--------------------|--------------------|
|              |                         | G               |       |                    |                       |                       |                       |                    |                      |                      |   |                    |                    |
| DLL 3        | 0                       | 2.295           | 2.48  | 7.5                |                       |                       |                       |                    |                      |                      |   |                    |                    |
| DLL 8        | 10                      | 2.285           | 2.48  | 7.9                | 4712.4                | 2690.6                | 4752.92               | 25                 | 10289.2              | 10339.1              | 49.9                                    | 31                 | 56                 |
| DLL 1        | 15                      | 2.284           | 2.48  | 7.9                | 4715.5                | 2696                  | 4760.58               | 28                 | 10293                | 10358.4              | 65.4                                    | 40                 | 68                 |
| DLL 2        | 20                      | 2.299           | 2.48  | 7.3                | 4706.8                | 2696.5                | 4743.82               | 25                 | 10295.1              | 10378.8              | 83.7                                    | 56                 | 81                 |
| CLL 6        | 0                       | 2.301           | 2.476 | 7.1                |                       |                       |                       |                    |                      |                      |   |                    |                    |
| CLL 5        | 10                      | 2.293           | 2.476 | 7.4                | 4704.3                | 2700.8                | 4752.39               | 32                 | 10298.4              | 10333.6              | 35.2                                    | 23                 | 55                 |
| CLL 8        | 15                      | 2.304           | 2.476 | 6.9                | 4705.6                | 2701                  | 4743.36               | 27                 | 10300                | 10360                | 60                                      | 42                 | 69                 |
| CLL 1        | 20                      | 2.319           | 2.476 | 6.3                | 4709.5                | 2710.9                | 4741.73               | 25                 | 10310.4              | 10386.6              | 76.2                                    | 59                 | 84                 |
| D5050 3      | 0                       | 2.291           | 2.469 | 7.2                |                       |                       |                       |                    |                      |                      |   |                    |                    |
| D5050 8      | 10                      | 2.303           | 2.469 | 6.7                | 4711                  | 2699.9                | 4745.49               | 25                 | 10297.6              | 10339.8              | 42.2                                    | 31                 | 56                 |
| D5050 1      | 15                      | 2.301           | 2.469 | 6.8                | 4702.1                | 2684.8                | 4728.3                | 19                 | 10285.8              | 10360                | 74.2                                    | 53                 | 72                 |
| D5050 6      | 20                      | 2.295           | 2.469 | 7.0                | 4708.5                | 2691                  | 4742.63               | 24                 | 10290.1              | 10377.6              | 87.5                                    | 61                 | 84                 |
| C5050 7      | 0                       | 2.301           | 2.463 | 6.6                |                       |                       |                       |                    |                      |                      |   |                    |                    |
| C5050 4      | 20                      | 2.289           | 2.463 | 7.1                | 4706.7                | 2690.8                | 4747.03               | 28                 | 10290                | 10336.4              | 46.4                                    | 32                 | 60                 |
| C5050 2      | 15                      | 2.302           | 2.463 | 6.5                | 4712.5                | 2700.2                | 4747.33               | 26                 | 10298                | 10364.6              | 66.6                                    | 50                 | 76                 |
| C5050 5      | 20                      | 2.301           | 2.463 | 6.6                | 4711.2                | 2702.3                | 4749.76               | 29                 | 10300.8              | 10388.7              | 87.9                                    | 65                 | 94                 |
| DGS 3        | 0                       | 2.273           | 2.461 | 7.6                |                       |                       |                       |                    |                      |                      |   |                    |                    |
| DGS 8        | 10                      | 2.302           | 2.461 | 6.5                | 4711.9                | 2689.8                | 4736.67               | 19                 | 10286.9              | 10338.3              | 51.4                                    | 39                 | 39                 |
| DGS 6        | 15                      | 2.296           | 2.461 | 6.7                | 4704.5                | 2680.8                | 4729.8                | 18                 | 10280.5              | 10354.5              | 74                                      | 54                 | 54                 |
| DGS 7        | 20                      | 2.278           | 2.461 | 7.4                | 4702.1                | 2677.6                | 4741.74               | 26                 | 10272                | 10361.8              | 89.8                                    | 59                 | 59                 |
| CGS 2        | 0                       | 2.288           | 2.462 | 7.1                |                       |                       |                       |                    |                      |                      |   |                    |                    |
| CGS 6        | 10                      | 2.281           | 2.462 | 7.4                | 4714.3                | 2695.6                | 4762.37               | 32                 | 10300.8              | 10329.8              | 29                                      | 19                 | 51                 |
| CGS 4        | 15                      | 2.269           | 2.462 | 7.8                | 4711.2                | 2679.2                | 4755.53               | 27                 | 10279.8              | 10344.4              | 64.6                                    | 40                 | 67                 |
| CGS 8        | 20                      | 2.288           | 2.462 | 7.1                | 4711.8                | 2686.6                | 4745.95               | 23                 | 10281.4              | 10387.2              | 105.8                                   | 73                 | 96                 |